# FIRST-PRINCIPLES STUDY OF MOLECULAR ADSORPTION OF HYDROGEN ON SODIUM ADATOM GRAPHENE

A

Dissertation

submitted to the Central Department of Physics, University Campus,

in the Partial fulfillment for the Requirement of

Master's Degree of Science in Physics


By

**KAMAL BELBASE**

**Central Department of Physics**

**University Campus, Tribhuvan University**

**Kirtipur, Kathmandu, Nepal**

November, 2013

# ACKNOWLEDGEMENT

I would like to acknowledge everyone who supported me through out this period of my dissertation, family and friends, and supervisors without whom I would not have been able to complete this work. I am indebted to my supervisors Dr. Narayan Prasad Adhikari and Mr. Nurapati Pantha for their constant aspiration and incredible assistance throughout this work. Their constant guidance had helped me to realize my potentials in this field ranging from computational techniques to bring out a fruitful analysis of my work. The patience that grew was awesome, which would not have been possible without their persistent encouragement. I would also like to thank Prof. Dr. Lok Narayan Jha and all entire family members of CDP for their support.

I would like to extend my acknowledgement to all my friends especially Mr. Asim Khaniya with whom I spent momentous long days laughing, teasing, and discussing. I would like to thank my seniors Mr. Anil Adhikari, Mr. Chiranjibi Bhattarai, and Mr. Saran Lamichhane for their support.

I would also like to acknowledge University Grants Commission (UGC) for their partial financial support.

I am, of course, very grateful to all my family members for their constant motivating love and support.

# RECOMMENDATION

It is certified that **Mr. Kamal Belbase** has carried out dissertation work entitled "**First-Principles Study of molecular Adsorption of Hydrogen On Sodium Adatom Graphene**" under our supervision and guidance.

We recommend the dissertation in partial fulfillment for requirement of Master's Degree of Science in Physics.

(Supervisor)

(Dr. Narayan Prasad Adhikari)
Central Department of Physics
Tribhuvan University, Kirtipur
Kathmandu, Nepal

Date : .....

(Supervisor)

(Mr. Nurapati Pantha)
Central Department of Physics
Tribhuvan University, Kirtipur
Kathmandu, Nepal

Date : .....


# EVALUATION

We certify that we have read this dissertation and in our opinion, it is good in the scope and quality as dissertation in partial fulfillment for the requirement of Master's Degree of Science in Physics.

## Evaluation Committee

Dr. Narayan Prasad Adhikari
(Supervisor)

Mr. Nurapati Pantha
(Supervisor)

Prof. Dr. Lok Narayan Jha
(Head)
Central Department of Physics
Tribhuvan University, Kirtipur
Kathmandu, Nepal

(External Examiner)

(Internal Examiner)

Date :.....

# List of Figures

# List of Tables

# Contents

# Abstract

We have performed the first-principles calculations to study the stability, geometrical structures, and electronic properties of pure graphene and Sodium atom adsorbed graphene system. We have also studied the adsorption of hydrogen molecules on pure graphene and Sodium decorated graphene. The calculations are performed under Density Functional Theory (DFT) with van der Waals (vdW) interaction in DFT-D2 level of approximation, implemented by the Quantum Espresso version 5.0.1. It is found that as the number of carbon atoms increases in the graphene sheets the ground state energy decreases linearly. The estimated value of binding energy per carbon atom of pure graphene sheet having 32 carbon atoms is 7.904 eV/atom which agrees within 0.60% to the previously reported value 7.91 eV/atom and within 1.59% to the value 8.03 eV/atom. From the adsorption energies of sodium atom on the different sites of graphene, hollow site found most favorable. The estimated adsorption energies of sodium atom adsorbed on 2×2, 3×3, and 4×4 supercell of graphene are -0.29 eV, 0.45 eV, and 0.79 eV respectively. We found that the sodium atom is not bound to the 2×2 supercell of graphene sheet, which agrees with previous report. The study of electronic properties of sodium decorated graphene shows that the conduction band and valence band are overlapped. For 4×4 supercell, the magnetic moment of isolated sodium atom and Na-graphene system are 1.00 $\mu_B$ and 0.24 $\mu_B$ respectively, which agrees with previously reported values 1.00 $\mu_B$ and 0.27 $\mu_B$ respectively. The adsorption energy per hydrogen molecule for the adsorption of one to seven numbers of H2 molecules in Sodium decorated graphene is within ( 0.023 - 0.192 ) eV/$H_2$. The study of adsorption of hydrogen molecules on the optimized structures of pure graphene and sodium decorated graphene system shows that sodium decorated graphene system can be use for hydrogen storage.

# Chapter 1

# INTRODUCTION

## 1.1 General consideration

Carbon is the sixth element in the Periodic Table. It has two stable isotopes. $12_C$ (98.9% of natural carbon) with nuclear spin $I$=0 and nuclear magnetic moment $\mu_n$=0, and $13_C$ (1.1% of natural carbon) with $I$=$\frac{1}{2}$ and $\mu_n$=0.7024 $\mu_N$ ($\mu_N$ is the nuclear magnetron). Like most of the chemical elements, it originates from nucleosynthesis in stars and plays a crucial role in the chemical evolution of the Universe. The carbon atom has six electrons, four of them is in the valence shell and can forms various allotropes [1].

Carbon allotropes can be divided into three classes according to the type of bonding among atoms. This type of bonding depends upon the interactions or mixing of atomic orbitals, commonly called hybridization, and new orbitals formed are referred to as hybrid orbitals. When all the carbon atoms have $sp^3$-hybridization, diamond structure are formed and in the case $sp^2$-hybridization one get graphitic materials. The third class of allotropes contains the amorphous carbons which consists of non-crystalline mixtures of $sp^2$-and $sp^3$-hybridized carbon atoms. Diamond and graphite, the two well known allotropes of carbon, were known from the ancient time. Fullerenes, the third form of the carbon, were discovered around 1985 and carbon nanotubes around 1991. The graphite and diamond are 3-dimensional, nanotubes are 1-dimensional and fullerenes are 0-dimensional allotropes of carbon [2], Figure [1.1]. Graphite may be viewed as a stacking of graphene sheets that stick together due to the van der waals interaction, which is much weaker than the in-plane covalent bonds. This physical property explains the graphic utility of the material:

when we write with a piece of graphite, i.e. when it is scratched over a sufficiently rough surface, such as a piece of paper, thin stacks of graphene sheets are exfoliated from bulk graphite and now stick to the surface. This is possible due to the weak van der waals interaction between the graphene sheets. Graphene is the best theoretically studied allotrope of carbon for more than 60 years. Theoretically graphene had already been studied in year 1947 by Wallace [3] but Practically, graphene was discovered in 2004 by group led by A. K. Geim and K. S. Novoselov (University of Manchester, UK) [4]. The Nobel Prize in physics 2010 was awarded jointly to A. K. Geim and K. S. Novoselov for "groundbreaking experiments regarding the two dimensional graphene".

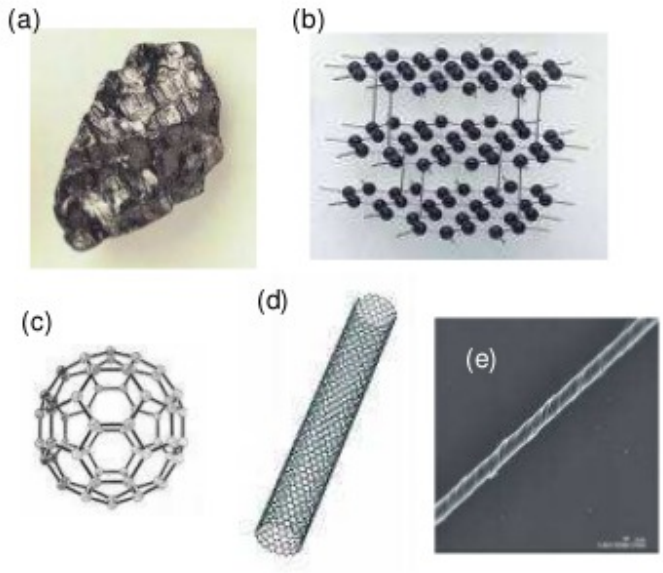


Figure 1.1: Graphitic allotropes (a) Piece of natural graphite. (b) Layered structure of graphite (stacking of graphene layers). (c) 0D allotrope: $C_{60}$molecule. (d)1D allotrope: single-wall carbon nanotube. (e) Optical image of carbon nanotube.

Graphene is a wonderful material with many superlatives to its name. It is the thinnest known material in the universe; it is the strongest, stiffest material we know and most stretchable crystal [5]. The unit cell of graphene is hexagonal cell with basis of two atoms and has lattice spacing 0.24 nm and area is 0.052 $nm^2$ [6]. The density of graphene is 0.77 $mg/m^2$ [6]. It is almost transparent, it absorbs only 2.3 % of the light intensity and independent of the wavelength in the optical domain. It exhibits a breaking strength of $\sim$ 42 N/m [5] and is about 100 times

stronger than the strongest steel. It conducts heat 10 times faster than copper [5] and can carry about 1000 times the current density than copper wire [7]. Graphene has been considered as a promising candidate for the post-silicon age [4, 8, 9]. It has enormous potential in the electronic device community, for example, field-effect transistor, transparent electrode, super small transistors, super dense data storage, increase energy storage and solar cell efficiency etc. Despite intense interest and remarkably rapid progress in the field of graphene-related research, there is still a long way to go for the widespread implementation of graphene. It is primarily due to the difficulty of reliably producing high quality samples, especially in a scalable fashion, and of controllably tuning the bandgap of graphene.

After the discovery of graphene, it has been extensively investigated and the idea of studying, structural and electronic changes that are induced by the adsorption of foreign atoms and molecules was exploited by researchers who were motivated both by technological and academic interest. Alkali metal (highly reactive chemical species) have a fairly simple electronic configuration and the adsorption on a graphite surface [highly oriented pyrolytic (HOPG)] have been investigated for the past 20 years. Adsorption is the process in which matter is extracted from one phase and concentrated at the surface of a second phase. The adsorption of different metal atoms on graphite and nanotube structures are of particular interest for catalysis, fuel cell technology and hydrogen storage [10].

Hydrogen storage is a key unsolved problem for producing fuel cells for hydrogen-powered automobiles or portable energy devices. Several different techniques like storage in tanks under high pressure, liquefying hydrogen at temperature below 20 K with an energetically expensive cooling system and forming metal or chemical hydrides have been developed to tackle this problem. These techniques, however, pose problems for practical use in automobiles: low hydrogen storage capacity, consumption of a great amount of energy to store or release hydrogen, limited number of cycling, and so on [11]. Since the first measurement of hydrogen uptake on carbon nanotubes, a number of research groups have focused their research on the use of carbon nanostructured materials, including nanotubes, as hydrogen storage materials due to their light weight and large surface area. There have been several optimistic reports claiming that at ambient conditions, hydrogen can be stored in carbon nanostructure materials well beyond 6% by weight, which used to be the

year 2010 target, but now is the 2015 (or beyond) target, set by the US Department of Energy for vehicular use. Moreover, it was reported that an appreciable amount of hydrogen could be stored only at $T < 80$ K under an ambient pressure up to 20 atm in carbon materials. The storage capacity of carbon nanotubes and graphitic fibers has been enhanced by doping alkali elements. The alkali atoms seem to have a catalytic effect in dissociating the $H_2$ molecule and promoting atomic adsorption. An advantage is that the doped systems can operate at moderate temperatures and ambient pressure [11].

In the present work, first-principles calculation were carried out to investigate the structural stability, electronic and magnetic properties of pure graphene layers and sodium adsorbed graphene systems. The first-principles approaches are widely used to study the electronic structure and to determine various physical properties of many electron systems [12]. They are based upon the fundamental laws of quantum mechanics and use variety of mathematical transformations and approximation techniques to solve the basic equations. The first-principles methods are widely used to study the electronic structure of solids and clusters. The first principles approaches mainly based on the Hartree-Fock approach, the DFT approach etc. The Hartree-Fock self consistent method is one-electron approximation in which the motion of each electron in the effective field of the other electrons is governed by a one electron Schrdinger equation [13]. In the Hartree-Fock approximation, the antisymmetric product of one-electron wave functions is used i.e it takes into account of the correlation arising due to electrons of same spin, however, the motion of the opposite spin remains uncorrelated. Beyond Hartree-Fock approximation, the methods which deals with the phenomenon associated with the many electron system are known as electron correlation methods. One of the first-principles method which take account of electron correlation is DFT, in which the electronic orbitals are solution to a Schrdinger equation which depends on the electron density rather than on individual electron orbitals. In this theory, the exchange-correlation is expressed as a functional of the electron density and the electronic states are solved for self-consistency as in the Hartree-Fock approximation. The exchange-correlation potential includes the exchange interaction arising from the antisymmetry of the wave functions and the dynamic correlation effect arising due to the Coulomb repulsion between the electrons. In principle, DFT theory is exact but it also treat the exchange and dynamic correlation effects approximately [12]. There are many com-

puter packages available to perform the first-principles calculations. Out of them, Quantum Espresso is one. In our present work, we have used Quantum Espresso to perform all the calculations.

## 1.2 Scope of the present work

In the present work, we have carried out the first-principles calculations to study the stability of pure graphene, stability, electronic, and magnetic properties of sodium atom adsorbed graphene system. We have also calculated the stability of hydrogen molecule adsorption on the sodium decorated graphene system. The calculations are performed under the DFT-D2 level of approximation, implemented with Quantum Espresso [14] package.

In chapter 2, we briefly describe general approximations used in Hartree-Fock (HF) method of calculation to find the ground state energy of many-electrons system. This theory generates the fermionic wave function that are anti-symmetric with respect to exchange of the two electron positions and includes the exchange between like spin electrons. The HF method takes account of interaction between electrons in an average way. The HF method of approximation does not take into account of the correlation effects due to the motion of the electrons having opposite spins. Then, we mainly deal with the Density Functional Theory (DFT), which take into account of electron correlation effects. As electron correlation methods, we discuss the DFT in which the exchange and correlation energy of many electrons system is expressed as a functional of the electron density.

In chapter 3, we discuss every details of our first-principles pseudo-potential based density functional calculations by using Quantum Espresso (QE) packages.

In chapter 4, we present the details of computational work performed under the density functional theory (DFT) with van der Waals i.e DFT-D2 level of approximation using the Quantum ESPRESSO package.

In chapter 5, we present and discuss the main findings of the present work. This chapter deals with the result of the first-principles calculation for:
• the ground state energy and equilibrium geometry of graphene sheets having the

number of carbon atoms 8, 18, 32, and 50.

• The adsorption energy, equilibrium distance between sodium atom and surface of graphene sheet, band structure, DOS, charge transfer, distortion of graphene sheet when sodium adsorbed.

•Also we present the equilibrium geometry of the hydrogen molecule adsorbed on the Na-graphene system.

In chapter 6, we recall our works with conclusions and concluding remarks.

# Chapter 2

# Density Functional Theory

## 2.1 General Consideration

Hartree-Fock (HF) theory account exchange interaction but it neglects correlation in the motion between two electrons with anti-parallel spins (i.e. correlation interaction). The exchange interaction is due to the Pauli exchange principle. In this case it states that if two electrons have parallel spins then they will not be allowed to sit at the same place at the same time. This phenomenon give rise to an effective repulsion between the electrons with parallel spins. This means that two electrons not only interacting by their charges but also by their spins.

The correlation interaction is also a result of Pauli exchange interaction. In this case there is a correlated motion between electrons of anti-parallel spins, which arises because of their mutual coulombic repulsion.

In Hartree-Fock (HK) approximation, it is assumed that in an atom with N-electrons each electrons moves in the field generated by the nucleus as well as remaining (N-1) electrons treated as overlapping charge clouds [13]. Therefore, this approximation reinforce each electron to see the average distribution of the other electron and not their instantaneous positions. Electron correlation in an atom is mainly caused by the instantaneous interactions between electrons. This means the Hartree-Fock (HK) approximation must be improved to account for electron correlations. Although, the Hartree-Fock wave function satisfies the anti-symmetry requirements of the Pauli's exclusion principle and hence includes the correlation effect arising from the electrons of same spin, the motion of electron with opposite spins remains

uncorrected. The difference of the exact non relativistic ground state energy of the system $\epsilon_0$ and HK energy $\epsilon_{HK}$ with the infinite basis set is called the correlation [13]. The expression for correlation energy can be written as

$$\epsilon_{corr} = \epsilon_0 - \epsilon_{HF}$$

In the present work, we just want to give a brief introduction on the development of Hartree-Fock approximation and its underlying assumption, which will help us to understand Density Functional Theory (DFT). In HF theory the multi-electron wave-function is expressed as slater determinant, which is constructed from a set of N single electron wave function. DFT also considers single-electron wave function. However, HF does indeed calculate full N-electron wave-function, where as DFT only attempts to calculate total electronic energy and overall electronic density distribution [15].

Any method that goes beyond the self consistent field (SCF) to consider the correlation between the motions of electrons is known as an electron correlation method. The underlying tenet of DFT is that any property of a system of many interacting particles can be regarded as a functional of ground-state density and there is a relationship between the total electronic energy and the overall electronic density. In addition, Thomas-Fermi model of a uniform gas and Slater local exchange approximation are the conceptual roots of DFT. DFT with general gradient approximation and plane wave as a basis set give appreciable results in many of the solid state physics calculations, which are comparable to experimental outcomes in low costs. After introducing exchange and correlation interaction on DFT, this method has played leading role for calculation of electronic and structural determination over conventional Hartree and Hartree-Fock models.

## 2.2 The Born-Oppenheimer approximation

This also known as adiabatic approximation. The problem is to find the solutions for Schrdinger equation of N electrons and M nuclei, that can be written as:

$$H_{tot}\psi(x_1, ....., x_N, \mathbf{R}_1, ....., \mathbf{R}_M) = E_{tot}\psi(x_1, ....., x_N, \mathbf{R}_1, .....\mathbf{R}_N) \qquad (2.1)$$

where the coordinates $x_i$ represent both the position coordinates, $r_i$, and the spin coordinates, $\sigma_i$, of the N electrons and the coordinates $R_i$ are the position coordinates

of the M atomic nuclei in the system. The Hamiltonian operator, $H_{tot}$, is given by:

$$\begin{aligned} H_{tot} &= -\frac{\hbar^2}{2m_e}\sum_{i}^{N}\nabla_i^2 - \sum_{I}^{M}\frac{\hbar^2}{2M_I}\nabla_I^2 \\ &\quad -\sum_{i}^{N}\sum_{I}^{M}\frac{Z_I e^2}{|\mathbf{r}_i - \mathbf{R}_I|} + \frac{1}{2}\sum_{i\neq j}^{N}\frac{e^2}{|\mathbf{r}_i - \mathbf{R}_j|} + \frac{1}{2}\sum_{I\neq J}^{M}\frac{Z_I Z_J e^2}{|\mathbf{R}_I - \mathbf{R}_J|} \end{aligned} \tag{2.2}$$

where $m_e$ is the mass of the electron and $M_I$ and $Z_I$ are respectively the mass and the charge (atomic number) of the nuclei. The first and the second term of equation [2.2] correspond to the kinetic energies of the electrons and nuclei, while the others represent the electron-nucleus, electron-electron, and nucleus-nucleus Coulomb interaction terms respectively.

It is clear that finding the ground state solution of the Schrdinger equation [2.1] with the Hamiltonian given by equation [2.2] is not an easy task. In fact, it is impossible to solve this equation exactly. A first approximation can be made when considering the large difference in mass between electrons and nuclei. The lightest nucleus, the proton, weights approximately 1836 times more than an electron. This means that the electron can adjust almost instantaneously to any changes in the positions of nuclei. Hence, the nucleus is supposed to be at rest in comparison to the motion of the electrons i.e. the electron moving in the field of fixed nuclei. The electronic wave function thus, depends only on the position of nuclei and not on their momenta. Also, the kinetic energy of the nuclei, second term of equation [2.2], which is inversely proportional with the nuclear mass $M_I$, is relatively small and can be neglected. Consequently, the nuclei can be considered as frozen and the nucleus-nucleus repulsion term becomes merely a constant, this constant to the operator only changes the phase of the eigenfunction and adds a constant term to the eigenvalue. Thus, nuclei can be treated adiabatically leading to a separation of the electronic and nuclear co-ordinates in the many body problem. Now, neglecting the terms containing the kinetic energy of nuclei and repulsion between nuclei total Hamiltonian of system equation [2.2] can be written as

$$\begin{aligned} H_{tot} &= -\frac{\hbar^2}{2m_e}\sum_{i}^{N}\nabla_i^2 + \sum_{i}^{N}\sum_{I}^{M}\frac{Z_I e^2}{|\mathbf{r}_i - \mathbf{R}_I|} + \frac{1}{2}\sum_{i\neq j}^{N}\frac{e^2}{|\mathbf{r}_i - \mathbf{r}_j} \end{aligned} \tag{2.3}$$

It is now possible to solve the equations [2.3] separately using the nuclear coordinates $\mathbf{R_I}$ as parameters. For convenience in notation, we will simply refer to $H_{tot}$ as H

and define $\hbar$ = e = m = 1 to get rid of all the constants in our notation (i.e. we switch to atomic units), so that

$$H = -\frac{1}{2}\sum_{i}^{N}\nabla_i^2 + \frac{1}{2}\sum_{i}^{N}\frac{1}{|\mathbf{r_i}-\mathbf{r_j}|} + \sum_{i}^{N}\sum_{I}^{M}\frac{Z_I}{|\mathbf{r_i}-\mathbf{R_I}|} \tag{2.4}$$

and the energy is expressed in hartree (1 hartree = 27.211 eV) and lengths in Bohr (1 Bohr = 0.529 Å ). The Hamiltonian [2.4] is completely determined by the number of electrons N, and the positions $\mathbf{R_I}$ and charges $Z_I$ of the nuclei. It stated in another way, the Hamiltonian is entirely specified through the third term of [2.4], i.e. the term originating from the nuclear potentials and the first two terms can be considered universal. A consequence of applying the adiabatic approximation to the Hamiltonian of equation [2.1] is the removal of the nuclear coordinates from the many particle wave function as given in equation [2.2]. The total energy is given as,

$$E_{tot} =< H_{tot} >=< H > +E_{nuc} =< T > + < V_{ee} > + < V_{ext} > +E_{nuc} \tag{2.5}$$

Where, the expectation values are taken with respect to $\psi_0(x_1.....x_N)$. This does not mean that the energy is independent of nuclear coordinates, but the interaction of electrons with the nuclei is only included as an interaction with the external potential is

$$V_{ext}(\mathbf{r}) = \sum_{I}\frac{Z_I}{|\mathbf{r}-\mathbf{R_I}|} \tag{2.6}$$

## 2.3 Density Functional Theory

As stated earlier, Hartree-Fock (HF) theory account exchange interaction but it neglects correlation in the motion between two electrons with anti-parallel spins (i.e. correlation interaction). To account electron correlation effects, we discuss the Density Functional Theory (DFT) in which the exchange-correlation is expressed as a functional of the electron density and the electronic states are solved for self-consistency as in Hartree-Fock approximation.

The density functional theory (DFT) is presently the most successfull (and also the most promising) approach to compute the electronic structure of matter. Its applicability ranges from atoms, molecules and solid to nuclei and quantum and classical fluids. In its original formulation, the DFT provides the ground state properties of system, and the electron density plays a key role. DFT can predicts a great variety

of molecular properties: molecular structures, vibrational frequencies, atomization energies, ionization energies, electric and magnetic properties, reaction paths, etc. Originally DFT has been generalized to deal with many different situations: spin polarized systems, multicomponent systems such as nuclei and electron hole droplets, free energy at finite temperatures, superconductors with electronic pairing mechanisms, relativistic electrons, time-dependent phenomena and excited states, bosons, molecular dynamics, etc.

The electron density n($\mathbf{r}$) is the probability to find any electron in certain volume element d$\mathbf{r}$. It is defined by square-integrating the wave-function over all spin coordinates and all space coordinates except the first one;

$$n(\mathbf{r}) = N \sum_{s_1} ... \sum_{s_N} \int ... \int |\psi(\mathbf{r}_1, \mathbf{s}_1, \mathbf{r}_2, \mathbf{s}_2, ...., \mathbf{r}_N, \mathbf{s}_N)|^2 d\mathbf{r}_1 .... \mathbf{r}_N \tag{2.7}$$

Since electrons are indistinguishable, the probability of finding any electron in d$\mathbf{r}$ is just N times the probability of finding 1 electron there. Theoretically it is a probability density, but it is more commonly called the electron density. The boundary conditions for n($\mathbf{r}$) thus have to be that it is positive for all $\mathbf{r}$, vanishes at infinity, and integrates to the total number of electrons N:

$$n(\mathbf{r}) \geq 0, \tag{2.8}$$

$$n(\mathbf{r} \to \infty) = 0, \tag{2.9}$$

$$\int n(\mathbf{r}) d\mathbf{r} = N. \tag{2.10}$$

Using the electron density as a basic variable, has several advantages compared to using the wave-function. First and foremost of all, it is a function consisting of only the 3 spatial variables instead of the 3N variables of the wave-function, thus having a tremendous computational advantage. Also, it is an observable, so unlike the wave-function it can be measured experimentally, for example by x-ray diffraction. At all the atomic sites, it has a finite maximum value due to the positive attraction located there.

The idea of using the electron density instead of the wave-function as a method to obtain information about the electronic structure is almost as old as the theory of quantum mechanics itself. Thomas and Fermi were amongst the first to independently develop a theory based on the density, in which they approximated the electron distribution using statistical model [16, 17].

### 2.3.1 Thomas-Fermi model

The Thomas-Fermi model (TF) assumes that electrons are distributed uniformly in the phase space, with two electrons in every $h^3$ of volume. Now, for each position of space volume element $d^3$r, we fill out a sphere of momentum space to the Fermi momentum $p_f$:

$$\frac{4}{3}\pi p_f^3(\mathbf{r}) \tag{2.11}$$

As the number of electrons must be the same in both position space and momentum space, we find for the electron density n($\mathbf{r}$):

$$n(\mathbf{r}) = \frac{8\pi}{3h^3}p_f^3(\mathbf{r}) \tag{2.12}$$

Solving for $p_f$ and using this to calculate the classical kinetic energy, we now get a relation of the kinetic energy as a functional of electron density:

$$T_{TF}[n] = C_F \int n^{\frac{5}{3}}(\mathbf{r})d^3\mathbf{r} \tag{2.13}$$

where, now in atomic units,

$$C_F = \frac{3}{10}(3\pi^2)^{\frac{2}{3}} \tag{2.14}$$

Neglecting the exchange and correlation terms, we can express the total energy of an atom in just the electron density,

$$E_{TF}[n] = C_F \int n^{\frac{5}{3}}(\mathbf{r})d^3(\mathbf{r}) - Z\int \frac{n(\mathbf{r})}{r}d^3\mathbf{r} + \frac{1}{2}\int \frac{n(\mathbf{r})n(\mathbf{r\prime})}{|\mathbf{r}-\mathbf{r\prime}|}d^3\mathbf{r}d^3\mathbf{r\prime} \tag{2.15}$$

where the first term is the local approximation to the kinetic energy and the last term is the classical electrostatic Hatree energy. TF theory was thus the first official density functional theory. It has major drawbacks however, as the exchange energy and electron correlation was totally neglected, resulting in a large error in the kinetic energy term. It was also proven that TF theory could not describe molecular bonding. Back then it was also not clear whether this DFT was fundamentally sound.

In 1964, Hohenberg and Kohn published a paper in which they mathematically prove the exactness and viability of using n($\mathbf{r}$) as opposed to the much more complex $\psi$ [18]. Because of the still unknown exchange and correlation and the major contribution from those to the kinetic energy, HK-DFT did not achieve a high accuracy in calculations. It was a year later, in 1965, that Kohn and Sham found a way of approaching this problem to good accuracy and thus created DFT in the form we know it today.

### 2.3.2 Hohenberg-Kohn Theorem

The starting point of any discussion of DFT is the Hohenberg-Kohn (HK) theorem [19]. It represents the most basic of a number of existence theorems which ensure that stationary many-particle systems can be characterized (fully) by the ground state density and closely related quantities. As the reasoning leading to the HK theorem is quite instructive, it is worthwhile to study this prototype of an existence theorem in some detail.

**The first Hohenberg-Kohn theorem** is stated as: The external potential $v(\mathbf{r})$ is a unique functional (within a trivial additive constant) determined by the electron density $n(\mathbf{r})$.

Therefore, as $v(\mathbf{r})$ fixes the Hamiltonian H, $n(\mathbf{r})$ also uniquely determines all other properties of the system. After 40 years, it has finally been rigorously proved that it is indeed physically justified to use the electron density $n(\mathbf{r})$ as a basic variable.

The original proof is actually very simple and is done by a *reductio ad absurdum*. Let $n(\mathbf{r})$ be the ground-state density for a system of N electrons in an external potential $v(\mathbf{r})$, which has the ground-state wave-function $\psi$ and the energy E. Then we can write for the energy,

$$E = < \psi|\hat{H}|\psi >$$

$$= \int v(\mathbf{r})n(\mathbf{r})d\mathbf{r} + < \psi|\hat{T} + \hat{V}_{ee}|\psi > \tag{2.16}$$

suppose that another potential $v'(\mathbf{r}) \neq v(\mathbf{r})+constant$ with ground state $\psi'$ results in the same density $n(\mathbf{r}$. $\psi'$ of course cannot be equal to $\psi$ as they are the solutions to different Schrdinger equations. Then

$$E' = \int v'(\mathbf{r})n(\mathbf{r})d\mathbf{r} + < \psi'|\hat{T} + \hat{V}_{ee}|\psi' > \tag{2.17}$$

Now the variational principle states that

$$E < \left\langle \psi'|\hat{H}|\psi' \right\rangle$$

$$= \int v(\mathbf{r})n(\mathbf{r})d\mathbf{r} + < \psi'|\hat{T} + \hat{V}_{ee}|\psi' > \tag{2.18}$$

$$= E' + \int [v(\mathbf{r}) - v'(\mathbf{r}]n(\mathbf{r})d\mathbf{r} \tag{2.19}$$

If we swap the prime and unprimed quantities, we find in the same way that

$$E < \left\langle \psi|\hat{H}|\psi \right\rangle \tag{2.20}$$

$$= E + \int [v'(\mathbf{r}) - v(\mathbf{r}]n(\mathbf{r})d\mathbf{r} \tag{2.21}$$

Adding (2.28) and (2.30) together this implies

$$E + E' < E + E' \tag{2.22}$$

This of course is a contradiction, which establishes the fact that there can only be one $v(\mathbf{r})$ that produces the ground-state density, and conversely that the ground-state density $n(\mathbf{r}$ uniquely determines the external potential $v(\mathbf{r})$.

Now, as it is proven that $n(\mathbf{r})$ contains all the necessary information for the entire system, it follows that all observables are certain functionals of $n(\mathbf{r})$. The total energy $E_v[n]$ and its constituents, the total kinetic energy $T[n]$, the total external potential energy $V_{ext}[n]$ and the total electron-electron interaction energy $V_{ee}[n]$ are now written as

$$E_v[n] = T[n] + v_{ext}[n] + V_{ee}[n] \tag{2.23}$$

Rewriting this in the form of

$$E_v[n] = \int v(\mathbf{r})n(\mathbf{r})d\mathbf{r} + T[n] + V_{ee}[n]$$

$$= \int v(\mathbf{r})n(\mathbf{r})d\mathbf{r} + \left\langle \psi|\hat{T} + \hat{V}_{ee}|\psi \right\rangle \tag{2.24}$$

we can see that integral part is system dependent. For the other part, which is universally valid, we define a new HK function as

$$F_{HK}[n] == \left\langle \psi|\hat{T} + \hat{V}_{ee}|\psi \right\rangle \tag{2.25}$$

$$= T[n] + V_{ee}[n]$$

so that equation (2.33) becomes

$$E_v[n] = \int v(\mathbf{r})n(\mathbf{r})d\mathbf{r} + F_{HK}[n] \tag{2.26}$$

Although this functional $F_{HK}[n]$ appears to be just another formulation, it is actually very important as it is applicable to each and every system. If it were known exactly, it would have been possible to solve the Schrdinger equation exactly, and there would have been no need of approximations. However, it contains the functionals for the kinetic energy $T[n]$ and the electron-electron interaction energy $V_{ee}[n]$, both of which the explicit forms are totally unknown. It can be convenient to extract the classical Coulomb energy from $V_{ee}[n]$ and write

$$F_{HK}[n] = \frac{1}{2}\int \frac{n(\mathbf{r})n(\mathbf{r}')}{|\mathbf{r}-\mathbf{r}'}d\mathbf{r}d\mathbf{r}' + G[n] \tag{2.27}$$

where $G[n]$ is a (unknown) universal functional containing the kinetic energy $T[n]$ and all the non-classical contributions.

To come back to the total energy $E_v[n]$, it is of course clear that for the correct $n(\mathbf{r})$ this quantity equals the ground-state energy $E_0$. Using the variational principle, it is easily shown that insertion of the correct $n(\mathbf{r})$ minimizes $E_v[n]$. Consider a trial density $n'(\mathbf{r})$ which satisfies the necessary boundary conditions $n'(\mathbf{r}) \geq 0$ and $\int n'(\mathbf{r})d\mathbf{r} = N$. As proven,$n'(\mathbf{r})$ has a unique wave-function $\psi'$. Taking the $\psi'$ as the trial wave-function for the Hamiltonian $\hat{H}$ corresponding to the real density $n_0$, we can write

$$\left\langle \psi'|\hat{H}|\psi' \right\rangle = \int v(\mathbf{r})n'(\mathbf{r})d\mathbf{r} + F_{HK}[n']$$

$$= E_v[n'] \geq E_0[n] = \left\langle \psi|\hat{H}|\psi \right\rangle,$$

or more compactly

$$E_0[n] \leq E_v[n'] \tag{2.28}$$

This density variational principle is also known as **the second Hohenberg-Kohn theorem** The HK functional $F_{HK}[n]$ delivers the lowest energy if and only if the input density is the true ground-state density $n_0$.
For the ground-state density we can minimize the energy functional by using the constraint that

$$\int n(\mathbf{r})d\mathbf{r} = N \tag{2.29}$$

Using the method of Lagrangian multipliers we can now write

$$\delta \left\{ E_v - \mu \left[ \int n(\mathbf{r} d\mathbf{r} - N \right] \right\} = 0 \tag{2.30}$$

the stationary principle which the ground-state density has to satisfy. Solving for $\mu$, we get the Euler-Lagrange equation

$$\mu = \frac{\delta E_v[n]}{\delta n(\mathbf{r}}$$

$$= v(\mathbf{r}) + \frac{\delta F_{HK}[n]}{\delta n(\mathbf{r})} \tag{2.31}$$

where $\mu$ turns out to be the chemical potential

### 2.3.3 The self-consistent Kohn-Sham equations

The Hohenberg-Kohn theorems allow us to rewrite the energy into two parts, the system dependent $\int v(\mathbf{r})n(\mathbf{r})d\mathbf{r}$ the unknown functional $F_{HK}[n]$. Directly applying this to real world problems, using explicit approximate forms for $T[n]$ and $V_{ee}[n]$ has its simplicities, as it creates equations that depend only on $n$, but the downside is that this method seemed to be greatly inaccurate. However, a year after the publication of Hohenberg and Kohn's paper, Kohn and Sham devised a better way to handle the unknown function $F_{HK}[n]$. They realized that most of the problems of direct density functional used before arise due to how they determine the kinetic energy and proposed a new method to indirectly approach $T[n]$. By doing this they turned DFT into a practical tool for real world calculations.

Kohn and Sham added orbitals (one electron functions) to create a non-interacting reference system from which the kinetic energy can be computed to good accuracy, leaving only a small correction to be calculated separately. To begin with, the exact formula for the kinetic energy for a set of orbitals is defined as

$$T = -\frac{1}{2} \sum_{i}^{N} n_i \langle \phi_i | \nabla^2 | \phi_i \rangle \tag{2.32}$$

with $\phi_i$ and $n_i$ the orbitals and their occupation numbers, and $0 \leq n_i \leq 1$. From the HK theory this energy is a functional of density,

$$n(\mathbf{r}) = \sum_{i}^{N} n_i \sum_{s} |\phi_i(\mathbf{r}, s)|^2 \tag{2.33}$$

However for an interacting system, there will be an infinite number of terms. This is hard to work with, and Kohn and Sham showed that it is possible to use simpler formulas to describe a non-interacting reference system, using the non-interacting Hamiltonian

$$\hat{H}_s = -\frac{1}{2}\sum_i^N \nabla_i^2 + \sum_i^N v_s(\mathbf{r}) \tag{2.34}$$

without the electron-electron interactions and for which the ground-state electron density is exactly $n(\mathbf{r})$. This system has kinetic energy

$$T_s = \langle\psi_s| - \frac{1}{2}\sum_i^N \nabla_i^2|\psi_s\rangle \tag{2.35}$$

Hartree-Fock theory already showed that for a non-interacting system like this one, the ground-state wave-function can be exactly represented by a determinant:

$$\psi_s = \frac{1}{\sqrt{N!}} det[\phi_1\phi_2.....\phi_N], \tag{2.36}$$

where the orbitals $\phi_i$ are the N lowest eigenstates of the one-electron Hamiltonian

$$\hat{h}_s\phi_i = \left[-\frac{1}{2}\nabla^2 + v_s(\mathbf{r})\right]\phi_i = \epsilon_i\phi_i \tag{2.37}$$

Here, $v_s$ is the non-interacting external potential. Using this, one can express the kinetic energy $T_s[n]$ and the electron density $n(\mathbf{r})$ as

$$T_s[n] = -\frac{1}{2}\sum_i^N \langle\phi_i|\nabla^2|\phi_i\rangle \tag{2.38}$$

$$n(\mathbf{r}) = \sum_i^N \sum_s |\phi_i(\mathbf{r}, s)|^2 \tag{2.39}$$

This non-interacting kinetic energy $T_s$ is of course still not the exact kinetic energy T, even if both systems have the same density. Kohn and Sham had the very good idea of rewriting the problem in such a way that $T_s$ does become the exact kinetic energy of that problem, simply moving the small residual part of the true kinetic energy $T$ to the heap of the non-classical contributions. In order to do this, the equation [2.25] can be written as

$$F_{HK}[n] = T_s[n] + J[n] + E_xc[n] \tag{2.40}$$

with the *exchange-correlation energy*, containing the small difference between $T$ and $T_s$ and the non-classical $V_{ee}$, defined as

$$E_{xc}[n] \equiv T[n] - T_s[n] + V_{ee}[n] - J[n] \tag{2.41}$$

For this system, we again minimize the energy using the constraint [2.31]:

$$\begin{aligned} 0 &= \delta \left\{ E_v - \mu \left[ \int n(\mathbf{r}) d\mathbf{r} - N \right] \right\} \\ &= \delta \left\{ \int v(\mathbf{r}) n(\mathbf{r}) d\mathbf{r} + T_s[n] + J[n] + E_{xc}[n] - \mu \left[ \int n(\mathbf{r}) d\mathbf{r} - N \right] \right\} \\ &= v(\mathbf{r}) + \frac{\delta T_s[n]}{\delta n} + \frac{\delta J[n]}{\delta n} + \frac{\delta E_{xc}[n]}{\delta n} - \mu \end{aligned} \tag{2.42}$$

Defining

$$v_{eff}(\mathbf{r}) \equiv v(\mathbf{r}) + \frac{\delta J[n]}{\delta n(\mathbf{r})} + \frac{\delta E_{xc}[n]}{n(\mathbf{r})} \tag{2.43}$$

and

$$v_{xc}(\mathbf{r}) \equiv \frac{\delta E_{xc}[n]}{\delta n(\mathbf{r})} \tag{2.44}$$

we thus get the Euler-Lagrange equation

$$\mu = v_{eff}(\mathbf{r}) + \frac{\delta T_s[n]}{\delta n(\mathbf{r})} \tag{2.45}$$

with the Kohn-Sham effective potential:

$$v_{eff}(\mathbf{r}) = v(\mathbf{r}) + \int \frac{n(\mathbf{r}')}{|\mathbf{r} - \mathbf{r}'|} d\mathbf{r}' + v_{xc}(\mathbf{r}) \tag{2.46}$$

As [2.45] is simply a rearrangement of [2.31].

The KS Euler-Lagrange equation [2.45] with the constraint [2.29] has the exact same form as the one obtained from conventional DFT, the only difference is that it applies to a system of non-interacting electron moving in the external potential $v_s(\mathbf{r}) = v_{eff}(\mathbf{r})$. Therefore, it is easy to obtain the $n(\mathbf{r})$ that satisfies [2.45], one just has to solve the N one-electron equations

$$\left[ -\frac{1}{2}\nabla^2 + v_{eff}(\mathbf{r}) \right] \phi_i = \epsilon_i \phi_i \tag{2.47}$$

and using the fact that

$$n(\mathbf{r}) = \sum_{i}^{N} \sum_{s} |\phi_i(\mathbf{r}, s)|^2 \tag{2.48}$$

(2.46-2.48) are the canonical Kohn-Sham equations.

As $v_{eff}$ depends on $n(\mathbf{r})$, $\phi_i$ depend on $v_{eff}$ and finally $n(\mathbf{r})$ depends on $\phi_i$, these self-consistent equations need to be solved iteratively. Usually one begins with a initial guessed $n(\mathbf{r})$, constructs a $v_{eff}$ from [2.46], solves for $\phi_i$ using [2.47] and finally gets a new $n(\mathbf{r})$ from [2.48]. This process continues until the density converges, at which time self-consistency is achieved.

As of now, all of the theory aforementioned has been exact and no approximations have been made to arrive here. Unfortunately, an explicit expression for $E_{xc}[n]$ has not been found, and we will have to resort to some approximations to be able to go further.

### 2.3.4 The exchange correlation functional

The main problem with the Kohn-Sham procedure described above is the introduction of the unknown exchange-correlation functional. As long as there is no expression for this term, it is impossible to solve the KS equations. Therefore, several approximations have been devised to get an explicit form for this functional. The most widely used approximation in solid state physics are the local density approximation (LDA) and the generalized gradient approximation (GGA). The idea behind the local density approximation is to assume that the $E_{xc}$ can be written in the following form.

$$E_{xc}^{LDA} = \int \rho_r \epsilon_{xc}(\rho(\mathbf{r}))d\mathbf{r} \tag{2.49}$$

where $\epsilon_{xc}(\rho(\mathbf{r}))$ is a functional that gives the exchange-correlation energy per particle of an electron gas of a uniform density $\rho(\mathbf{r})$. At first sight, it would seem that LDA is not very accurate since the density of any real system is far from homogeneous but in practice it seems to work surprisingly well. LDA can be regarded as the zeroth order approximation of the exchange-correlation functional. When gradient

corrections are added to this approximation, as:

$$E_{xc}^{GGA}[\rho] = \int \epsilon_{xc}(\rho(\mathbf{r}), |\nabla\rho(\mathbf{r})|, ...)d\mathbf{r} \tag{2.50}$$

We get the so-called generalized gradient approximations (GGA). There are a lot of different exchange-correlation functionals of the GGA type which are based on both physical *ab-initio* insights and empirical data. In general, one can say that GGA improves on LDA when it comes to calculating bond lengths and energies, but for some systems where GGA fails, LDA leads to correct results because of some hazardous error cancellations.

### 2.3.5 Solution of the Kohn-Sham equations: Self-consistency iteration procedure

In Kohn-Sham equation of the system, we need to know first the wave functions that constructed the electronic density $\rho(\mathbf{r}$. These wave functions are solutions of Kohn-Sham equation which means the estimated solution of Kohn-Sham equations must be known before it can be solved. The problem can be solved iteratively by several step. The electronic density is constructed from the wave functions. From the Kohn-Sham equation to obtain the electrostatic Coulomb potential, we must construct and solve the Poisson's equation. The diagonalization involves unknown coefficient given by:

$$(H - \epsilon S)c_{ij} = 0 \tag{2.51}$$

which is the result of one particle eigenvalues with their corresponding coefficients $c_{ij}$ of expansion. The corresponding wave function can be expanded as $\psi_i(\mathbf{r}) = \sum_j c_{ij}\phi_i(\mathbf{r})$, which are then used to construct the electronic density $\rho(\mathbf{r})$. This constructed electron density is called the output electron density. This is to say that taking as input an initial density, a new density is found. This new density is then fed into the equation system which yields an output density and so on. This is repeated self-consistently until the output density is the same as the input density. This is known as the self-consistency field cycle (SCF). The resulting density is used to calculate the total energy of the system $E[\rho(\mathbf{r})]$ and the forces $F_{\mathbf{r}} = -\frac{\partial E}{\partial \mathbf{r}}$ acting on the atoms of the system. It is important to keep in mind that the main source of inaccuracy in DFT is normally a result of the approximate nature of the exchange-correlation functional.

## 2.4 Density functional theory with van der Waals (vdW) correction

In principle DFT is exact but in practice, approximations must be made for how electrons interact with each other. These interactions are approximated with so called exchange-correlation (XC) functionals and much of the success of DFT stems from the fact that XC functionals with very simple forms often yield accurate results. However, there are situations where the approximate form of the XC functional leads to problems. One prominent example is the inability of exchange-correlation functionals to describe long-range electron correlations that are responsible for van der Waals (vdW, dispersive) interaction. The van der Waals (vdW) interactions can be viewed as an attractive inter- actions originating from the response of electrons in one region to instantaneous charge density fluctuations in another. The leading term of such an interaction is instantaneous dipole-induced dipole which gives rise to the well known -$\frac{1}{r^6}$ decay of the interaction energy with inter-atomic separation r.

The lack of dispersion forces, van der Waals (vdW) forces, is one of the most significant problems with modern DFT and the quest for DFT-based methods which accurately account for dispersion is becoming one of the active field of research in computational chemistry, physics, and materials science. Many DFT-based dispersion techniques have been developed and The most widely applied and very well tested method is DFTD [20], which proved high accuracy in many different applications [21, 22]. The basic requirement for any DFT-D approach is that it yields reasonable -$\frac{1}{r^6}$ asymptotic behavior for the interaction of particles, where r is the distance between the particles. A simple approach for achieving this is to add an additional energy term which accounts for the missing long range attraction. Then the total energy becomes,

$$E_{tot} = E_{DFT} + E_{disp} \tag{2.52}$$

where $E_{tot}$ is the total DFT energy with a given exchange correlation functional and $E_{disp}$ is the dispersion interaction given by,

$$E_{disp} = -\sum_{i,j} \frac{c_6^{i,j}}{r_{i,j}^6} \tag{2.53}$$

where the dispersion coefficients $c^{i,j}$ depends on elemental pairs i and j. Within this approach dispersion is assumed to be pairwise additive and can therefore be calculated as a sum over all pairs of atoms i and j. Because of the simplicity and low computational cost this pairwise $\frac{C_6}{r^6}$ correction scheme is widely used. But this scheme also has some shortcoming which limits the accuracy one can achieve with it. The dispersion term includes only the leading term of correction and neglects the many-body dispersion. the next drawback is that the $\frac{C_6}{r^6}$ function diverges for small separations (small r) and this divergence must be removed.

The widely applicable method of deriving the dispersion coefficients, referred as DFT-D2 scheme [23], is published by Grimme in 2006. In this approach the dispersion coefficients are calculated from a formula which couples ionization potentials and static polarizabilities of isolated atoms.

In the present work, we have used the density functional theory with van der Waals interactions in DFT-D2 approach, the first-principles calculations performed to study the adsorption of sodium atom on graphene, hydrogen molecule on pure graphene and hydrogen molecule on sodium decorated graphene. The inclusion of van der Waals forces in the DFT-D2 approach plays the key role in the study of physisorption states, especially in gas adsorption. The adsorption of hydrogen molecule on pure graphene and sodium decorated graphene can be accounted by the attractive long-range van der Waals interactions.

# Chapter 3

# QUANTUM ESPRESSO

## 3.1 General Consideration

Quantum ESPRESSO (QE), is - an acronym for Quantum-opEn-Source Package for Research in Electronic Structure, Simulation, and Optimization is a multi-purpose and multi-platform package which contains a number of codes useful for many first-principles electronic structure calculations [14]. It is an integrated suite of computer codes for electronic structure calculations and materials modeling at the nanoscale. It builds on the electronic structure codes PWscf, PHONON, CP90, FPMD and Wannier. It is based on density-functional theory, plane waves, and pseudo-potentials (both norm-conserving and ultra-soft).

The QE distribution contains the core packages PWscf (Plane-Wave Self-consistent Field) and CP (Car-Parrinello) for the calculations of electronic-structure properties within Density-Functional Theory(DFT), using a Plane-Wave (PW) basis set and pseudo-potentials. The QE package usages plane wave basis sets for the expansion of electronic wave function, a pseudo-potential description of the electron-ion interaction, and DFT for the description of electron-electron interaction [18]. It is useful to calculate:

-the ground state energy and Kohn-Sham orbitals for both insulators and metals, in any crystal structure, for many exchange-correlation functionals,

-the structural optimization and variable cell molecular dynamics,

-the atomic forces and stresses,

-free-energy surface calculation at fixed cell through meta-dynamics.

Density-Functional Perturbation Theory (DFPT) can be use in the package to calculate the energy derivatives and related quantities [24]. We use the QE packages as our first-principles code. QE is a full *ab initio* package implementing electronic structure and energy calculation, linear response methods (to calculate phonon dispersion curves, dielectric constants, and Born effective charges) and third-order anharmonic perturbation theory. QE also contains two molecular-dynamics codes, CPMD (Car-Parrinello Molecular Dynamics) and FPMD (First-Principles Molecular Dynamics). Among them PWscf is the code that we have used to perform total energy calculations. PWscf uses both norm-conserving pseudo-potentials (PP) and ultrasoft pseudo-potentials (US-PP), within DFT.

In our case, the package based on DFT, plane wave basis set and PP with required contents were used in first-principles method of calculations to find total energies and converged geometries of pristine graphene, sodium adatom graphene, and hydrogen adsorption on sodium adatom graphene system. In addition, we have used this package in order to calculate band structure, density of states (DOS), from which we can predict the nature of material like insulator, semiconductor or metallic. We have also used this package to calculate charge transfer from adatom to graphene, from which we can predict about the nature of bonding between adatom and graphene.

## 3.2 Main Components of Package

This package is freely distributed and it contains main three components integrated together into a single frame work for input, output data and share same installation mechanism with large common code basis.

### 3.2.1 PWscf

PWscf developed by S.Baroni et al. [24], this code implements the iterative approach to self consistent using a plane wave basis set and both norm conserving and ultrasoft pseudo-potential (PP) method, using different matrix diagonalization methods.

This code also utilize the LDA and GGA exchange correlation functionals, including spin polarization. The main feature of PWscf calculation is self consistent calculations, structural relaxation, Electronic structure calculation, variable cell molecular dynamics and Nudged Elastic Band (NEB) calculation are performed by invoking executable file called **pw.x**. In addition, important feature include a possibility to calculate a phonon dispersion curve at desire value of wave vector for complex structural calculations (using DFPT) and other phonon related calculations. Their knowledge will help to study the crystal stability.

Among these the most important parameters in the input files of QE, we have:

• ibrav: This give the information about the Bravais lattice of structure. ibrav = 4, refer to hexagonal lattice, which we are using in our calculation. There are different types of specification ranging from ibrav = 1 to 14 to address 14 different kinds of Bravais lattice. For ibrav = 0 we must specify the lattice parameter in vector form.

• celldm (i)(i = 1, 2, 3): specifies the lattice parameters of the crystal and are given in atomic units, whereas i = 4, 5, 6 are the cosines of the angles between each pair of lattice vectors. In our case, celldm(1) = a, celldm(3) = $\frac{c}{a}$, where a, b and c (for hexagonal structure a = b) are the lattice vectors along X, Y and Z direction respectively.

• ecutwfc : The energy cutoff (in Ry) for the plane-wave basis. This value truncate the plane wave during the calculation. Since, after this value of cutoff energy the convergence will not affect. Larger values of ecutwfc increase accuracy, but calculation will take longer. In our case, we select ecutwfc from convergence test.

• nat: specifies the number of atoms in the unit cell. In our case, unit cell contain 2, 2×2 supercell contain 8, 3×3 supercell contain 18 carbon atoms.

• ntyp: represent the number of types of atomic species.

• nspin : if nspin = 2, the code will perform a spin-polarized calculation. This is important if we are dealing with a material with a magnetic moment. In spin-polarized calculations, each band energy is computed once for spin-up electrons and once for

spin-down electrons, meaning calculation take twice as long. If we set nspin = 1, indicate the crystal is non-magnetic.

• ATOMIC SPECIES: in this section we specify the symbols of the atoms, their corresponding masses (in amu) and the name of the files containing the pseudo-potentials (PP). The first entry on each line is the element's chemical symbol, the second is the atomic mass (in amu), and the third is the name of the file containing the PP (the file's location is controlled by the pseudo-dir parameter in the CONTROL namelist).

• ATOMIC-POSITIONS : each line contains the chemical symbol of one atom and the coordinates of that atom. Units are controlled by what is in parentheses following the header ATOMIC-POSITIONS. 'alat' means we are using Cartesian coordinates, everything is scaled by celldm(1). Other options are 'bohr' (using absolute Cartesian coordinate in units of Bohrs), 'angstrom' (using absolute Cartesian coordinates in units of Angstroms), or 'crystal'(the coordinate are in units of the lattice vectors of primitive cell). In case of cubic cell using crystal and using alat result in the same coordinates.

• K-POINTS : number of k-points, measures how well our discrete grid has approximated the continuous integral over the Brillouin Zone. Larger the value of k-points increase the accuracy but calculation take longer time to run. Generally k-points taken from convergence test. In our case, we take 15 for unit cell, 7 for 2×2 supercell, 5 for 3×3 supercell respectively.

**Postproc**

The PostProc module contains number of codes integrated together for post processing, that will help us to do the analysis of data file produced by PWscf calculation. This indeed utilizes following codes:

• **bands.x**: This extracts the files from PWscf calculation and records its eigenvalues at different K-points with corresponding energies values.

• **plotband.x**: This utilizes the files produced by bands.x and produce different file that helps in plotting entire band structure.

• **dos.x**: This helps to calculate electronic density of states at different kpoints.

• **projwfc.x**: This helps to calculate projections of wave function over atomic orbitals that performs population analysis and calculates projected density of states (PDOS), which help us to predict the contribution of density of states due to different atomic orbitals like s, p, d, f etc.

• **pp.x**: This help us for data analysis and plotting. The code performs two steps (1) reads the output file produced by 'pw.x', extract and calculate the desire quantity (2) writes the desired quantity to file in a suitable format for various types of plotting.

# Chapter 4

# Computational Methodology

## 4.1 General consideration

We have carried out the first-principles calculations to investigate structural stability of graphene, sodium adatom graphene and hydrogen adsorbed on Na-graphene system. We have also calculated electronic and magnetic properties of sodium adsorbed graphene system. The calculations are performed in the framework of the Density Functional Theory (DFT) with van der Waals interaction under the generalized gradient approximation (GGA) of Perdew, Burke, and Ernzerhof (PBE) [41] (to account electronic exchange and correlation effects) and self consistent plane wave pseudo-potential [34, 35, 36], implemented with the Quantum Espresso-5.0.1 package [14]. Throughout this calculations we have chosen Rappe-Rabe-Kaxiras-Joannopoulos (RRKJ) ultra-soft pseudo-potential to present the interaction between ion cores and valence electrons of all species (C, Na, H). The semicore ($2p3s$) sates of Na, ($1s$) state of hydrogen and ($2s2p$) states of carbon atom are treated explicitly as valence in the pseudo-potential description of the corresponding atoms.

First we have performed the relaxation calculations to obtain the optimize structure. In this calculation, system was allowed to fully relax using BFGS (Broyden-Fletcher-Goldfarb-Shanno) scheme until the total energy changes between two consecutive self consistent field (scf) steps is less than $10^{-4}$ Ry and force acting is less than $10^{-3}$ Ry/Bohrs.

After the relax calculations we have performed the self consistent calculation. Graphene is two dimensional crystal having hexagonal primitive unitcell with basis of two car-

bon atoms, so during the self consistent total energy calculations the Brillouin zone of graphene is sampled in the reciprocal space using the Monkhorst-Pack scheme with a appropriates number of mesh of k-points. The mesh of k-points determined from the convergence test. Smearing was to aid convergence. We have used of the 'Marzarri-vanderbilt' method or cold smearing with a small Gaussian spread of 0.001 Ry. Furthermore, we have chosen 'david' diagonalization method with the mixing factor 0.6 for self consistency.

In the computational calculations using Quantum Espresso, the first step is the construction or generation of crystal structure. we started our work with generation of unitcell of the graphene.

## 4.2 Generation of crystal structure

Graphene is a two dimensional single atomic layer of carbon atoms arranged in a Honeycomb lattice. In Quantum Espresso code [14], our first step was the generation of crystal structure through unitcell with Bravais lattice structure. In case of graphene, we have taken hexagonal primitive unitcell with the basis of two atoms, Figure [4.1]. The experimentally observed value of carbon-carbon distance is 1.42 Å [33] and it is used initially for the determination of atomic positions in unitcell. In QE, we have used hexagonal unitcell by mentioning 'ibrav = 4' in the input file. When we mentioned 'ibrav = 4', it automatically construct the hexagonal unitcell by using the three different vector which are given in equation (4.2). Some others parameters that has to be specified are: celldm(1) = $a$, celldm(2) = $\frac{b}{a}$ and celldm(3) = $\frac{c}{a}$, $a$, $b$ and $c$ are lattice constants in Bohrs along X, Y and Z-direction respectively. In case of hexagonal cell $b = a$, so celldm(2) = 1. In the input file the 'ATOMIC SPECIES' of different atoms are mentioned with their corresponding mass and respective pseudo-potential. For e.g. carbon atom (C) in the input file is mentioned as 'C 12.01 C.pbe-rrkjus.UPF' with atomic mass 12.01 amu and ultrasoft pseudo-potential C.pbe-rrkjus.UPF. The Figure [4.1] shows how we constructed the unitcell with carbon-carbon distance $a$ and lattice vectors

$$V_1 = a(1, 0, 0)\ V_2 = a(-\frac{1}{2}, \frac{\sqrt{3}}{2}, 0)\ and\ V_3 = a(0, 0, \frac{c}{a}) \tag{4.1}$$

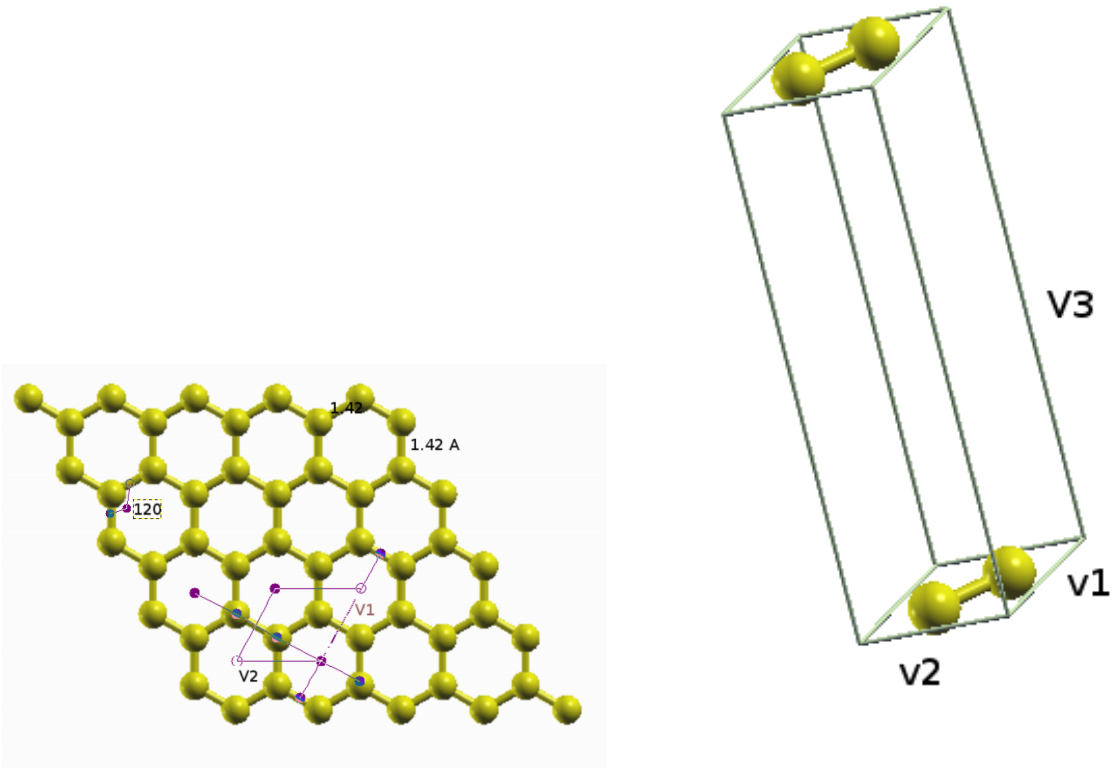


Figure 4.1: The construction of the unitcell. $V_1$ and $V_2$ are the lattice vectors along X and Y direction respectively. The bond length between carbon atoms is 1.42 Å and bond angle is $120^o$.

To implement these structure in our QE code the three important parameters in the input file namely kinetic energy cut off for the plane wave (ecutwfc), lattice parameter (a) and k-points has to be determined. These parameters are calculated from the convergence test i.e. convergence of the total energy with respect to these parameters, individually. The process to determine these parameters are discussed here in brief.

### 4.2.1 Kinetic energy cut off (ecutwfc)

The plane wave self-consistent code field (PWscf) implemented in the Quantum Espresso [14] expand the electron wave-function in terms of the infinite basis function that are plane waves. The value of the kinetic energy corresponding to the cutoff value of the basis function is called the kinetic energy cutoff. It is expressed in unit

of the energy Ry or eV. The plane wave expansion in the reciprocal space is

$$\psi_k(\mathbf{r}) = \frac{1}{\Omega}\sum_G C_{k.G} \exp i(k+G).\mathbf{r} \tag{4.2}$$

In principle, we need infinite numbers of plane wave but in order to reduce the computational cost we have to truncate the plane wave expansion from some acceptable value. To make the plane wave expansion (equation 4.2) finite, we truncated according to the condition

$$\frac{|k+G|^2}{2m} \leq E_{cut} \tag{4.3}$$

To find the value of ecutwfc, we run the 'sh' file (it is a file format which can execute many pw.x executable file for 'scf' calculation gradually). When we executed this file, we have fixed celldm(1) = 2.46 Å and k-points mesh at (15×15×1) with different value of the ecutwfc (i.e 20, 25, 30, 35, 40) Ry. At these different values of ecutwfc, we found different scf total energy. We plot a graph between the scf total energy and ecutwfc as shown in the Figure [4.2]. In the Figure [4.2], we look for the convergence of the total energy with respect to the value of the ecutwfc and we have chosen that value of the ecutwfc as the appropriate, from which the convergence of the total energy starts to occur. In our case, the kinetic energy cutoff was found to be 35 Ry. Now, for all further calculations we have used ecutwfc as 35 Ry. When we have the ecutwfc then we can predict about ecutrho (charge density cutoff). The value of ecutrho depends on what kind of pseudo-potentials we used. In our case, we have used ultra-soft pseudo-potentials so ecutrho = 10×ecutwfc. When we have the 'ecutwfc', we going to find the k-points mesh for unitcell.

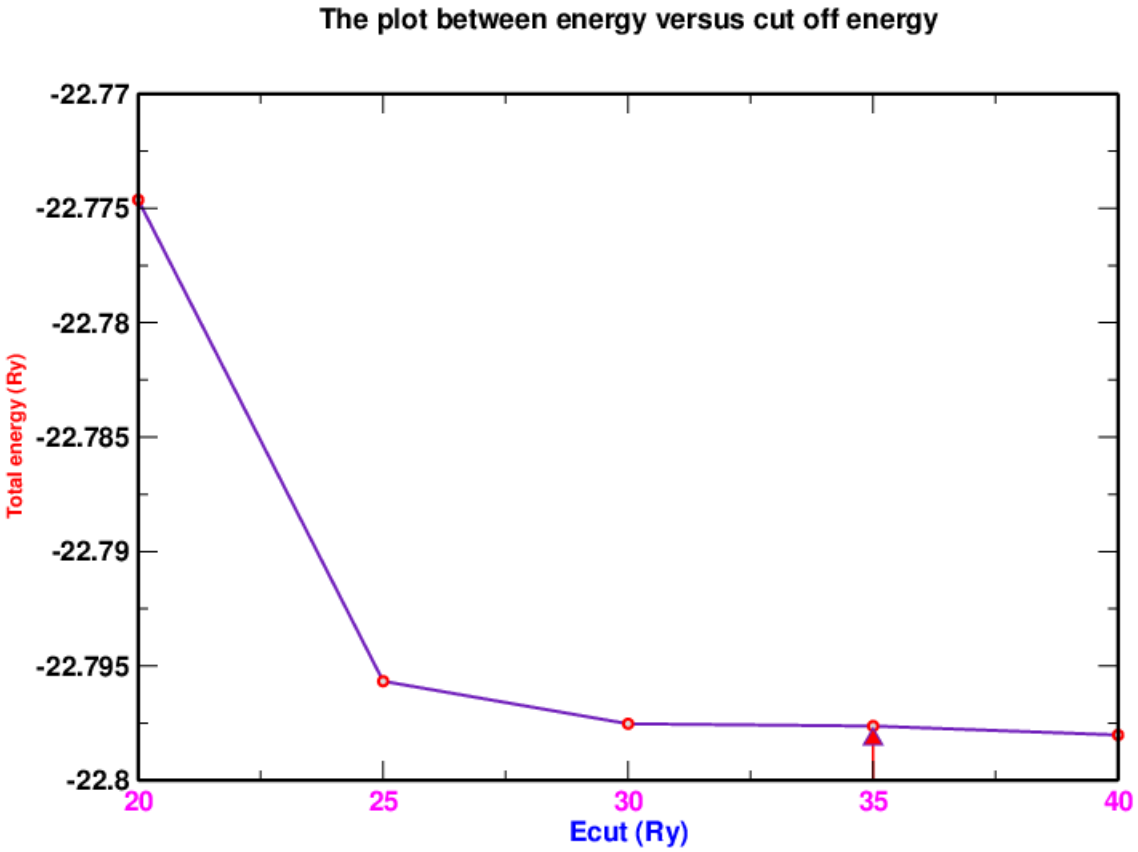


Figure 4.2: The total energy versus the kinetic energy cutoff for the unitcell: energy (Ry) along Y-direction and ecut along X-direction. From figure after 30 Ry, the total energy is almost constant so ecutoff = 35 Ry is appropriate for the further calculations. We can choose the value beyond 35 Ry but it increase computational time.

### 4.2.2 K-points

When we have ecutwfc, we use this value to find k-points mesh. Again we use 'sh' file with lattice parameter 2.46 Å and ecutwfc at 35 Ry for different k-points value i.e 6, 8, 10, 12, 14, 16, 18, 20. This 'sh' format file itself generates one scf input file by using one set of k-point values at one time. At every k-points value we obtained scf total energy. We have plotted a graph between total energy and k-points as in Figure [4.3]. By checking the convergence of energy, the appropriate value of k-point is taken from which total energy started to converge. From Figure [4.3], we take k-point value for our calculation is 15 for unitcell. We can use even denser k-points grid by increasing k-point value but these calculations take longer time to run. Similarly, the k-points value taken as 8, 5 and 4 for 2×2, 3×3 and 4×4 supercell respectively. After finding the 'ecut' and 'k-points mesh' we going to find out lattice constant for unitcell having two carbon atoms.

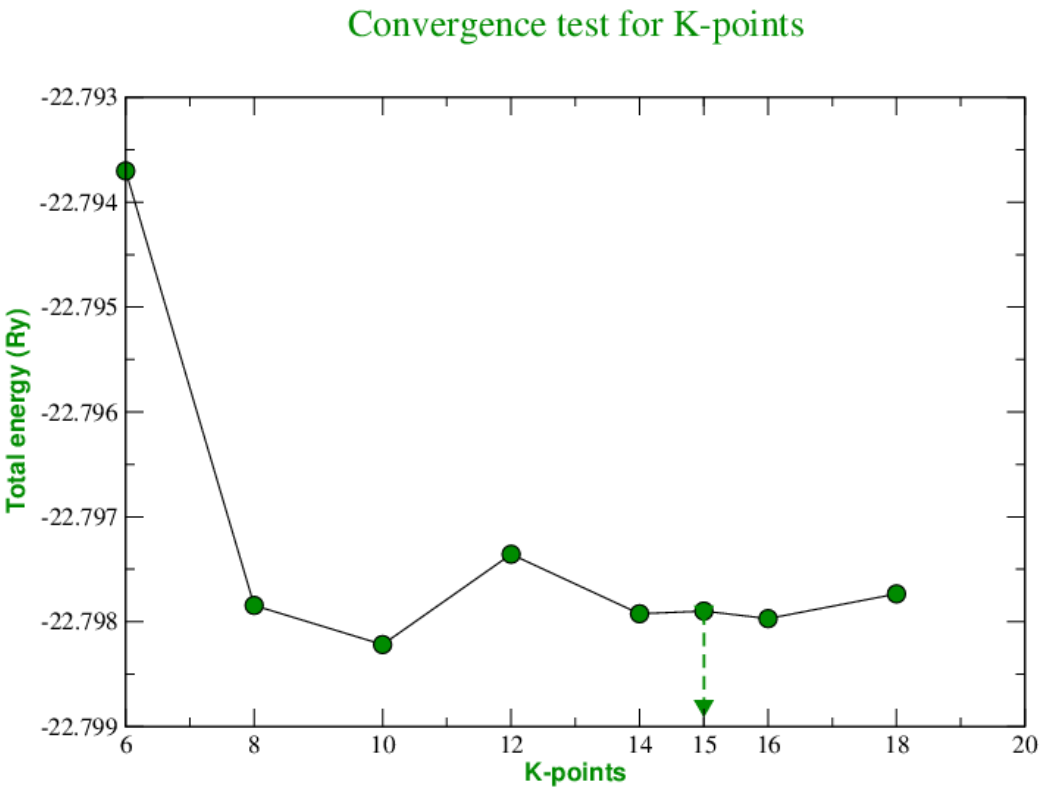


Figure 4.3: The graph is energy(Ry) versus kpoints. Energy is along Y-direction and k-points along X-direction. From graph it is seen that the energy is almost constant when k-point is at 15. So, in our case, we have chosen the k-point mesh of 15×15×1 for unitcell.

### 4.2.3 Lattice constant

We use the value of the ecutwfc (at 35 Ry) and k-point mesh (15×15×1) from above calculations to find the value of the lattice constant (i.e.celldm(1) or a). For this calculation also, we have made the 'sh' format file to run the scf calculation for different values of lattice parameter (4.50, 4.55, 4.60, 4.65, 4.70, 4.75, and 4.80) Bohrs. When we executed input file, we found different values of scf total energy at different values of lattice parameter. Then we plot the graph between the total energy and lattice parameter as shown in the Figure [4.2.3]. From Figure [4.2.3], we have taken the suitable value of lattice parameter at which the total energy becomes minimum. In our calculation, the value of the lattice parameter was found to be 4.65 Bohrs for unitcell containing two carbon atoms. The lattice parameter depending upon the number of carbon atoms per unitcell like 8, 18, and 32 atoms in the unitcell the lattice parameters are 9.30, 13.95, and 18.60 Bohrs respectively. This value of the lattice constant of the unitcell containing two carbon atoms is same as the experimental value of 2.46 Å[27].

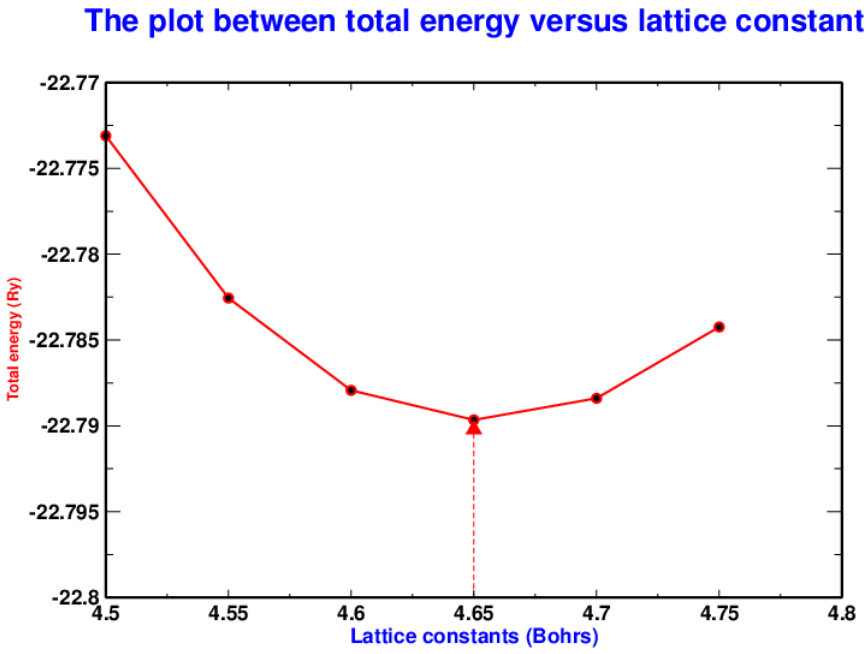


Figure 4.4: This is the plot between total energy of unit cell as a function of lattice parameter. In this plot energy is along Y-direction and lattice constant along X-direction. The plot shows that energy is minimum when dimension of unit cell is 4.65 Bohrs or 2.46 Å.

Once we have the unitcell of the pure graphene and three different parameters:

ecutwfc, lattice parameter and k-point mesh we performed the relaxation calculation of the unitcell to obtain optimized geometry. From the optimized geometry of unitcell, the distance between two nearest carbon atom is 1.42 Åwhich is same with the experimental value 1.42 Å[37]. When we have the unitcell, we repeated them in the $xy-$plane to obtain supercell of pure graphene, like 2×2 supercell of graphene is obtain by repeating two unitcell along X direction and two along Y direction. The Figure [4.2.3] shows the 4×4 supercell of graphene that constructed from the unitcell. After the relaxation calculation we have performed the 'scf' calculation to obtain the total energy of the system. Then the stability of pure graphene sheet was studied using the information obtained from scf and relax calculations. After calculations of the pure graphene, we adsorbed the sodium atom on pure graphene of different supercell.

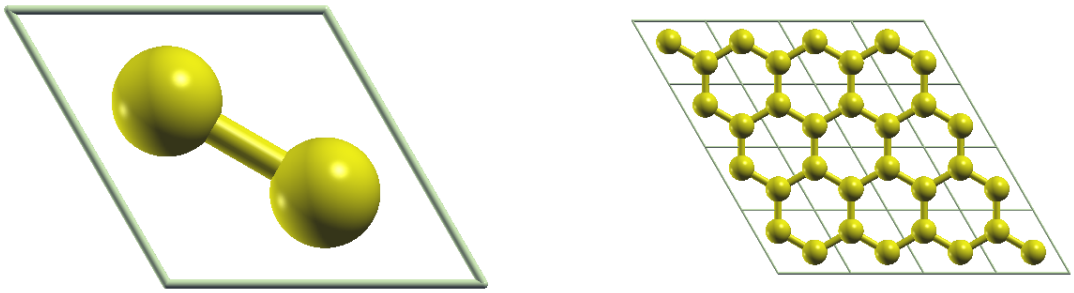

Figure 4.5: The figure shows the unitcell and 4×4 supercell of graphene.

The sodium adatom graphene system is modeled using single adatom in 2×2, 3×3, and 4×4 hexagonal graphene supercell containing 8, 18, and 32 carbon atoms respectively. This combination corresponds to the coverage of 1 adatom per 8, 18, and 32 carbon atoms.

The computer code uses a periodic supercell method due to which adatom-adatom interaction is not negligible, in order to avoid their interactions the length (vacuum length) of supercell has to make large enough. The height of supercell known as

vacuum length. The Figure [4.6] shows the variation of the energy of the 3×3 supercell of pure graphene with vacuum length.

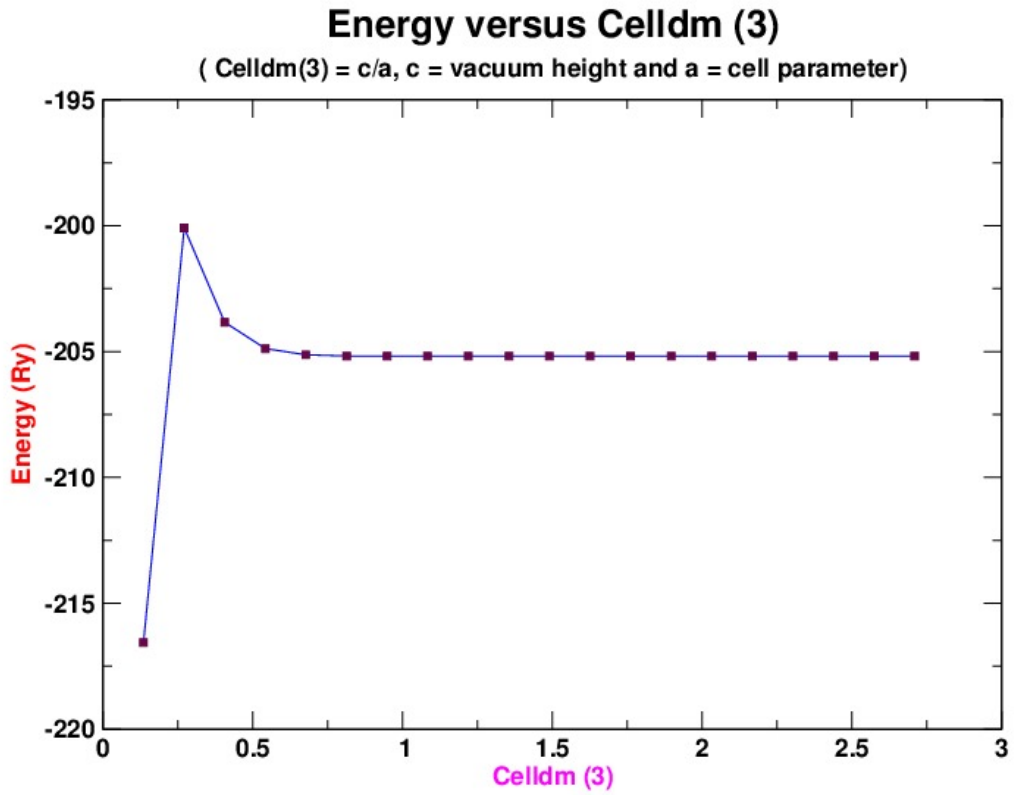


Figure 4.6: The variation of the energy with respect to celldm(3), which gives the vacuum length. Celldm(3) $=\frac{c}{a}$, $c$ is the vacuum length and $a = 13.95$ Bohrs is the lattice parameter for 3×3 supercell. This graph show that above 17.43 Bohrs we can choose any value for vacuum length, which fairly agree with result [28].

The adsorption of the sodium atom on the optimized graphene is allowed on three different sites of high symmetry: the hollow (H) site at the center of a hexagon, the bridge (B) site at the midpoint of a carbon−carbon bond, and the top (T) site directly above a carbon atom, Figure [4.7]. In the relax calculation, each adsorption site of the adatom−graphene system, the adatom is allowed to relax along the Z−direction in considered supercell of the graphene and ions of carbon atoms (C) in graphene allowed in all directions until forces on ions are less than $10^{-3}$ Ry/Bohrs. After the optimization of system we have prepared an input file for scf calculations by using relaxed coordinates of system to obtain total energy of the system. The

relax and scf calculations were performed by executable 'pw.x'. From the information of relax and scf output files we tested the stability of system and obtained their geometrical structures. To calculate adsorption energy of adatom graphene system, we also require the total energy of an isolated sodium and carbon atom in the consider supercell, which is calculated by considering single atom in the volume of supercell and only the Γ point of Brillouin zone is sampled.

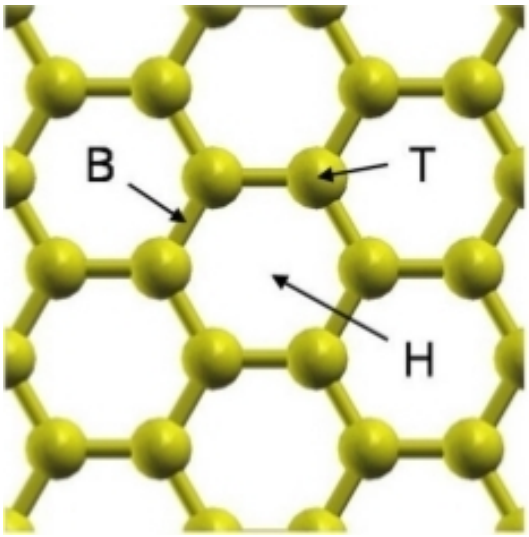


Figure 4.7: The three adsorption sites considered in the present work:hollow (H), bridge (B), and top (T)

We have also calculated Density of State (DOS) of the pure graphene and sodium decorated graphene system. In this calculation first of all we have performed 'scf' and 'nscf' calculation. During 'nscf' calculation we used more denser k-point mesh in order to obtain smooth density of states. These calculations were performed using the executable 'pw.x'. Then, we performed dos and projections of wave-functions over atomic orbitals (pdos) calculation using executables 'dos.x' and 'projwfc.x'.

We have calculated the band structures of pure graphene and sodium decorated graphene system. For bands calculations we took 100 k-points along specific direction of irreducible Brillouin zone in order to obtain fine band structure. In the Figure [4.8], gamma-K-M represent the irreducible Brillouin zone. It is the smallest part of the primitive Brillouin zone. For band structure, first we execute 'pw.x' and then 'bands.x'. To obtain the figure of bands structure we executed 'plotband.x'.

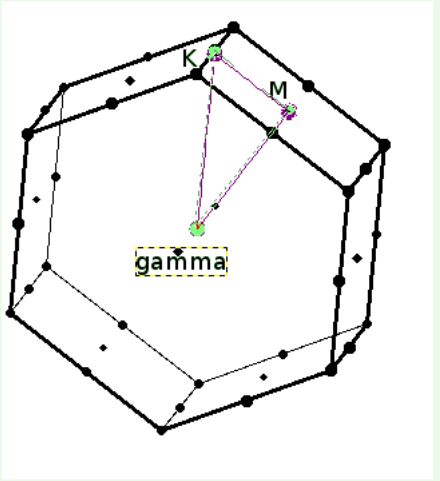


Figure 4.8: The figure shows the first Brillouin zone of hexagonal and triangular part gamma-K-M represent the irreducible Brillouin zone.

Further, we have performed first-principles study of the hydrogen adsorption on the optimized structure of sodium decorated graphene. This system is modeled by the adsorption of molecular hydrogen in a single sodium adatom graphene. First of all, we have performed the relax calculation by allowing the atomic positions to relax until the convergence is attained. Then we used these relax coordinates of the system to performed 'scf' calculation, from which we obtained the total energy. Similarly pure graphene and hydrogen molecules are also allowed to relax using the supercell of same dimension. For hydrogen adsorption process we have used single sodium atom decorated 3×3 supercell of graphene containing 18 carbon atoms. We increased the numbers of hydrogen molecule from one and calculated its adsorption energy. Also, we compared our calculated values with available experimental and theoretical values.

# Chapter 5

# Results and Discussion

## 5.1 General consideration

This chapter mainly focuses on the results and the interpretation of the present works. We have carried out the calculations to obtain the ground state energy, binding energies and equilibrium configurations of pure graphene sheet with 8, 18, 32, and 50 number of carbon atoms. We have also carried out the calculations to study the adsorption of sodium atom (Na) on the pure graphene sheets. To understand the electronic and magnetic properties of our system, we have performed the band structure calculations, density of state (DOS) and charge transfer calculations. Further, we have extended our work to investigate hydrogen storage capacity of sodium decorated graphene system. The calculations have been carried out within the framework of the Density Functional Theory (DFT) with van der Waals interaction i.e DFT-D2 level of approximation, implemented with the Quantum Espresso (QE) code of version 5.0.1 [14]. The obtained results are compared with the available experimental and theoretical results.

## 5.2 Results and Discussion

We have presented the results of the first-principles calculations carried out to obtain:

- Structure and Stability of pure graphene sheet

- Stability and structural geometry of Na adsorbed graphene
- Charge transfer calculations of Na adsorbed graphene
- Band structure calculations of pure graphene and Na adsorbed graphene
- Density of states of pure graphene and Na adsorbed graphene
- Stability of adsorption of hydrogen on Na decorated graphene

## 5.3 Structure and Stability of pure graphene sheet

In this section, we describe the study of the equilibrium configurations of the pure graphene sheet having the number of carbon atoms 8, 18, 32 and 50 in 2×2, 3×3, 4×4, and 5×5 supercell of graphene respectively, see Figure [5.1, 5.2, 5.3, 5.4].

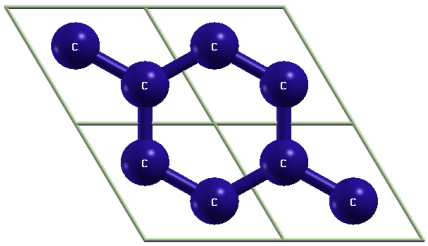

Figure 5.1: 2×2 supercell of graphene

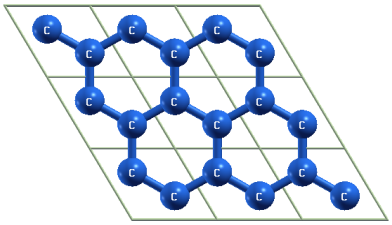

Figure 5.2: 3×3 supercell of graphene

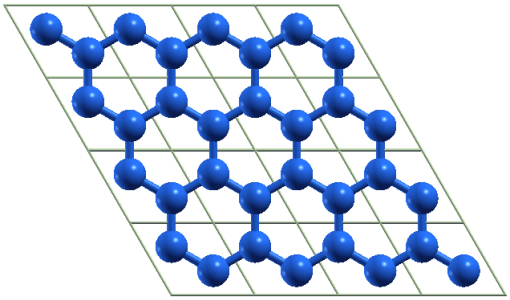

Figure 5.3: 4×4 supercell of graphene

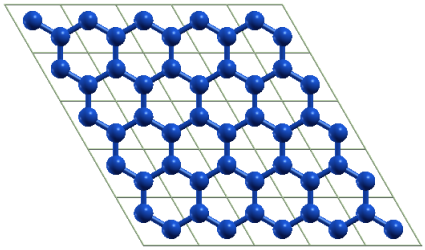

Figure 5.4: 5×5 supercell of graphene

We define the binding energy of graphene as

$$\Delta E = NE_C - E_G \tag{5.1}$$

where $\Delta E$ is the binding energy of the system, $E_G$ is the ground state energy of graphene, $E_C$ is the ground state energy of the isolated carbon atom in the considered supercell system, N is the number of carbon atoms in graphene sheet. Positive binding energy means system bound. Similarly, the binding energy per carbon atom can be estimated by using following formula

$$\triangle E_{percarbon} = \frac{NE_C - E_G}{N} \tag{5.2}$$

We have performed the relax calculations for the pure graphene sheet with 8, 18, 32, and 50 number of carbon atoms to obtain the optimized structure. We have also carried out the 'scf' calculations to obtain the total energy (ground state energy) of the system. To calculate binding energy of pure graphene, we also require the total energy of an isolated carbon atom, which is calculated by considering single carbon atom in the volume of supercell. The binding energy and binding energy per carbon atom are calculated by using Formula [5.1] and [5.2] and their values are listed in the Table [5.1].

Table 5.1: The ground state energy, binding energy and binding energy per carbon atom for the graphene sheet having 8, 18, 32, and 50 carbon atoms.

.

| Number of carbon atoms | Energy (Ry) | B.E. of carbon atom (eV) | B.E. per carbon atom ($\frac{eV}{atom}$) |
|---|---|---|---|
| $C_8$ | -91.192 | 62.315 | 7.789 |
| $C_{18}$ | -205.178 | 142.218 | 7.901 |
| $C_{32}$ | -364.768 | 252.945 | 7.904 |
| $C_{50}$ | -569.941 | 395.112 | 7.902 |

From Table [5.1], the binding energy and binding energy per carbon atom increases but ground state energy decreases as number of carbon atoms increases in the graphene sheet. Binding energy per carbon atom is almost same for the graphene sheet having 18 or more than 18 carbon atoms.

The variation of ground state energy of pure graphene sheet with the number of carbon atoms are shown in Figure [5.5].

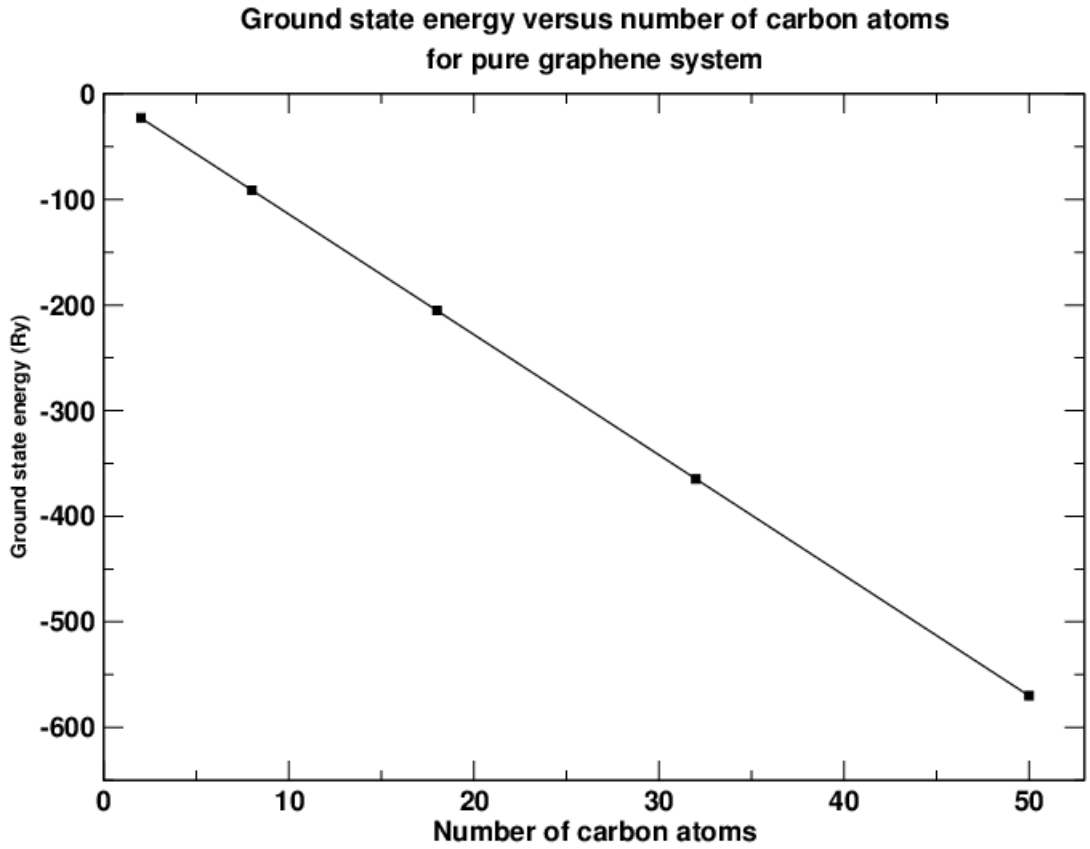


Figure 5.5: The variation of ground state energy with number of carbon atoms. The ground state energy decreases as the number of carbon atoms increases.

From the Figure [5.5], as the number of carbon atoms increases in the graphene sheet the ground state energy decreases linearly.

We have studied the variation of binding energy of graphene sheet with number of carbon atoms, Figure [5.6].

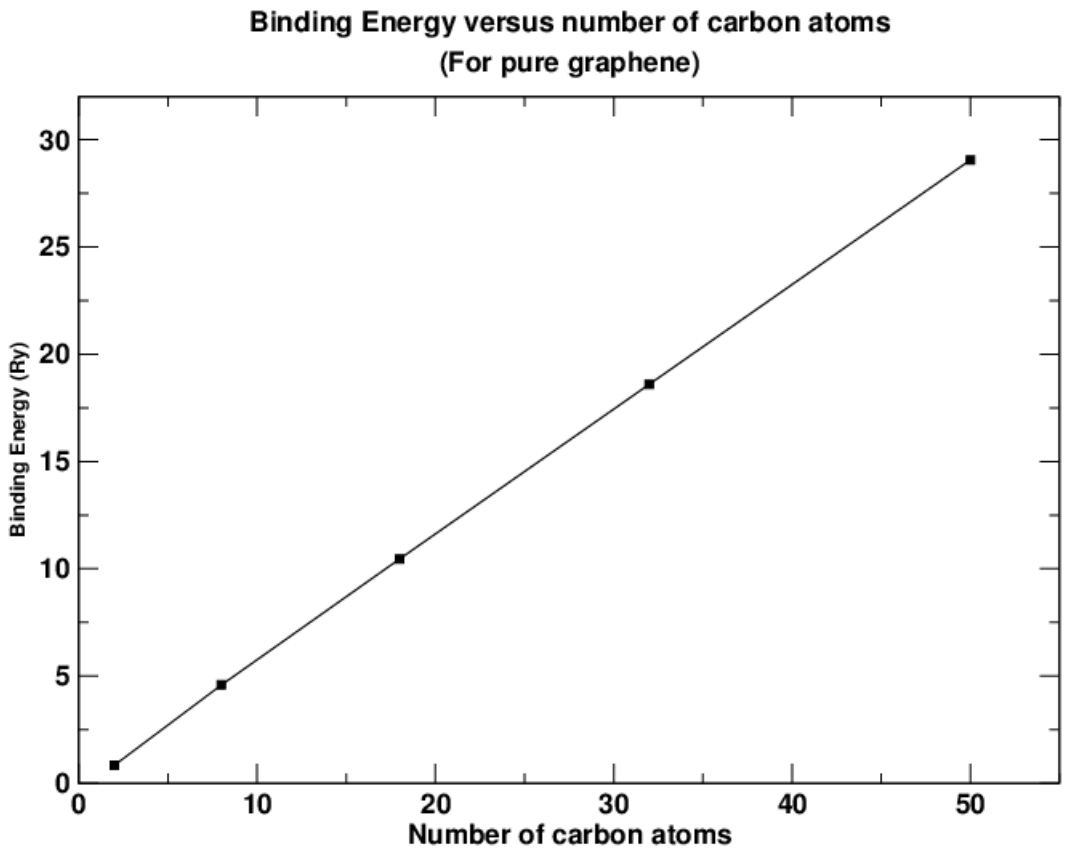


Figure 5.6: The variation of binding energy with number of carbon atoms of the pure graphene sheet. The binding energy of graphene sheet increases with number of carbon atoms increases.

Figure [5.6] shows that as the number of carbon atoms increases the binding energy of system increases. Therefore, the graphene sheet with large number of carbon atoms is more stable than less number of carbon atoms.

We have also studied the variation of binding energy per carbon atom of graphene sheet with number of carbon atoms, Figure [5.7].

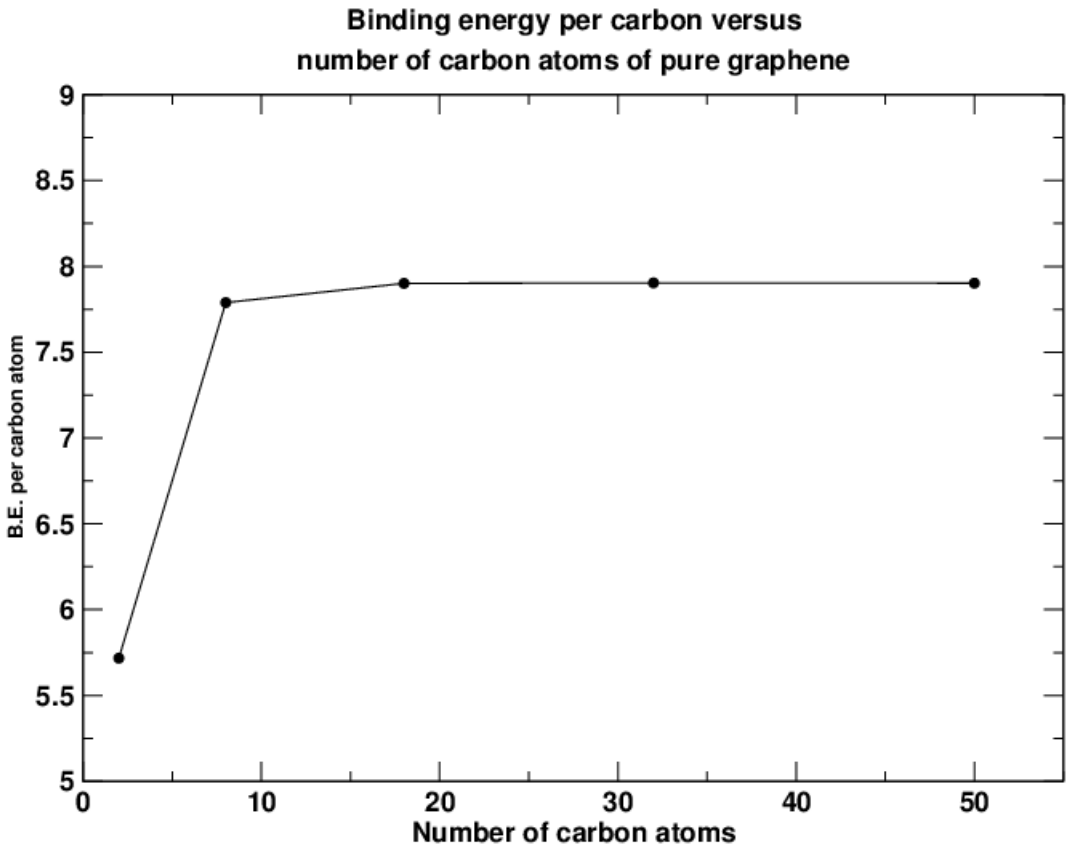


Figure 5.7: The variation of the binding energy per carbon atoms with number of carbon atoms. The binding energy per carbon atom for graphene sheet with 18 or more carbon atoms is almost constant.

The binding energy per carbon atom for 2×2 supercell of graphene, containing 8 carbon atoms, the value is 7.789 eV/atom. Similarly, for 3×3, 4×4, and 5×5 supercell of graphene the binding energy per carbon atom are 7.901 eV, 7.904 eV, and 7.902 eV respectively. The binding energy per carbon atom for pure graphene sheet with 18 or more number of carbon atoms is almost same, Figure [5.7]. Therefore, the graphene layer with 18 or more carbon atoms is more stable than that of lower size. The value of the binding energy per carbon atom of the pure graphene sheet with 32 carbon atoms agrees within 0.6% to the previously reported value 7.910 eV/atom [29] and within 1.59% to the value 8.03 eV/atom, reported by Oli et al [10].

## 5.4 Stability and structural geometry of Sodium (Na) atom adsorbed graphene

We have studied the adsorption of the sodium atom on the three sites of the high symmetry of the pure graphene sheets: hollow (H) site at the center of a hexagon, the bridge (B) site at the midpoint of a carbon-carbon bond, and the top (T) site directly above a carbon atom as shown in Figure [4.7].

We have considered the binding of sodium atom on three highly symmetric positions (H, B, and T). For each adsorption site the adatom and carbon atoms relaxed in three directions X, Y, and Z until the total energy change is less than $10^{-4}$ Ry between two consecutive scf steps and the force acting in each direction is less than $10^{-3}$ Ry/Bohrs. The binding energy (adsorption energy) of sodium atom on graphene sheet is calculated by using the relation

$$\Delta E = E_{Na} + E_G - E_{G+Na} \tag{5.3}$$

where $E_{Na}$ is ground state energy of sodium atom, $E_G$ is the ground state energy of graphene system and $E_{G+Na}$ is the ground state energy of sodium adatom graphene system. The positive binding energy means stability of the system. The total energy of an isolated sodium atom and graphene layer are calculated in 2×2, 3×3, and 4×4 supercell as that of total adatom graphene system. Out of the three adsorption sites, the site with the largest adsorption energy (minimum total energy) is referred to as the favored site for adsorption.

From the positions of the atoms after relaxation, we have obtained adsorption geometry. The adatom height (h) is defined as the difference in Z coordinates of adatom and the average of the Z coordinates of the carbon atoms in the sodium-graphene system. we have also calculated the distance ($d_{Ac}$ ) between the adatom and its nearest carbon atom. In case of sodium adsorption, the distortion produce in the graphene sheet is very small. The distortion is measured from the difference of average Z coordinates of carbon atoms before and after sodium atom adsorbed. The distortion is also measured from change of dihedral angle. In the present work, the sodium adatom graphene system is modeled using single adatom in the 2×2, 3×3, and 4×4 supercell of graphene which contains 8, 18, and 32 number of carbon atoms respectively.

### 5.4.1 Calculations in 2×2 supercell

2×2 supercell is the repetition of unitcell two times along X-direction and Y-direction as shown in Figure [5.8]. It has 8 carbon atoms.

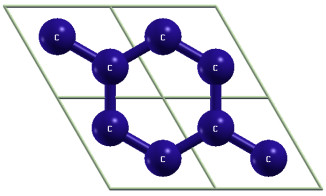

Figure 5.8: 2×2 supercell of graphene. There are two unit-cells along X direction and two unit-cells along Y direction.

We have investigated the adsorption of the sodium atom on three different sites: hollow (H), bridge (B), and top (T) as shown in Figure [5.9, 5.10, 5.11]. For this study, sodium atom was kept at the distance of 2.39Å , 2.51Å , 2.40Å from graphene sheet at H, T, and B positions respectively. To estimate the adsorption of graphene (2×2) and sodium atom, we have carried out the relax calculations under DFT-D2 level of approximation.

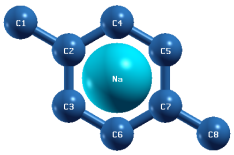


Figure 5.9: Adsorption of sodium at hollow (H) site

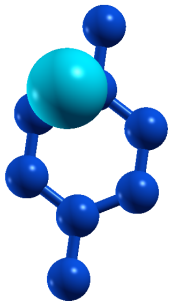

Figure 5.10: Adsorption of sodium at bridge (B) site

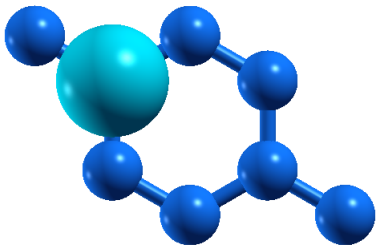

Figure 5.11: Adsorption of sodium at top (T) site

From our investigation, we have found that the ground state energies of sodium adatom graphene systems are -183.450 Ry, -183.443 Ry, and -183.443 Ry for the sodium atom in the H, B, and T sites of graphene respectively. This shows that the H site is the most favorable as it has lower energy than that of Na in B and T sites of graphene. The ground state energy of Na atom is -92.280 Ry and the ground state energy of pure graphene is -91.191 Ry in the same size of supercell. The adsorption energy of sodium atom in the sodium-graphene system is computed by using formula [5.3]. In the Table [5.2], we have presented the values of the adsorption energy, the equilibrium distances between the adatoms and graphene sheet, the adatom height (h), the distance between the sodium atom and nearest carbon atom ($d_{AC}$) and the distortion of graphene sheet.

Table 5.2: Energetic and structural properties for the hollow (H), bridge (B), and top (T) sites for the sodium atom considered in this work. The properties listed are the binding energy ($\triangle$E), adatom height (h), adatom-carbon distance ($d_{AC}$), and graphene distortion ($d_{GC}$)

| Atom | site | $\triangle$E (eV) | h ($\mathring{A}$) | $d_{AC}$ ($\mathring{A}$) | $d_{GC}$ ($10^{-2}$ $\mathring{A}$) |
|---|---|---|---|---|---|
| Na | Hollow | -0.29 | 2.40 | 2.79 | -1.04 |
| | Bridge | -0.38 | 2.52 | 2.50 | -1.36 |
| | Top | -0.38 | 2.51 | 2.54 | -1.33 |

From Table [5.2], it is seen that the adsorption energy of sodium atom in the sodium-graphene is negative which signifies that the sodium is not bound to the graphene sheet having 8 carbon atoms ( 2×2 supercell). This result agrees with previous results [28].

We have also analyzed all the bond lengths, bond angles and dihedral angles of the graphene sheet before and after the sodium atom adsorbed in the hollow site. In case of pure graphene sheet, the bond length (C-C), the bond angle (C-C-C), and dihedral angle (C-C-C-C) is 1.42 Å, 120.00, and $0.00^o$.

Figure [5.12] shows the optimized geometry of the sodium-graphene system. From Figure [5.12], the C-C bonds (1C-2C, 7C-8C) have the bond length of 1.419 Å whereas the C-C bonds in the hexagonal ring (2C-4C, 4C-5C, 5C-7C, 7C-6C, 6C-3C, 3C-2C) have the bond length of 1.423 Å. This shows that the C-C bond length, out of the hexagonal ring, shortened. The maximum change of bond length is 0.002 Å.

The bond angles formed by carbon atoms (2C-4C-5C, 4C-5C-7C, 5C-7C-6C, 7C-6C-3C, 6C-3C-2C, 3C-2C-4C) are $120.00^o$. When sodium atom adsorbed on graphene, bond angles do not change.

When Na adsorbed on graphene, the graphene sheet gets distorted. From Table [5.2], the distortion produced by sodium atom in the graphene sheet is small. The negative values of distortion of graphene sheet signifies that the sodium atom pushed the graphene sheet downwards. Also, the distortion of graphene sheet due to adsorption of sodium atom can be measure in term of change of dihedral angle. The dihedral angles for (2C-4C-5C-7C, 4C-5C-7C-6C, 5C-7C-6C-3C, 7C-6C-3C-2C, 6C-3C-2C-4C, 3C-2C-4C-5C) do not change. Which signifies that all the carbon atoms (2C-3C-6C-7C-5C-4C) on the hexagonal ring remain in the same plane. Similarly, the change of dihedral angles for (1C-2C-3C-6C, 1C-2C-4C-5C, 4C-5C-7C-8C, 8C-7C-6C-3C, 6C-3C-2C-1C, 5C-4C-2C-1C) is maximum. The maximum change in dihedral angle is $0.210^o$.

From our study, it is seen that the Na atom on the Na-graphene system remains in the hollow position such that it is equidistant from all the carbon atoms (2C-3C-

6C-7C-5C-4C) on the hexagonal ring as shown in Figure [5.12]. Also, all the bond lengths of hexagonal ring are increases slightly but bond angles remain unchanged.

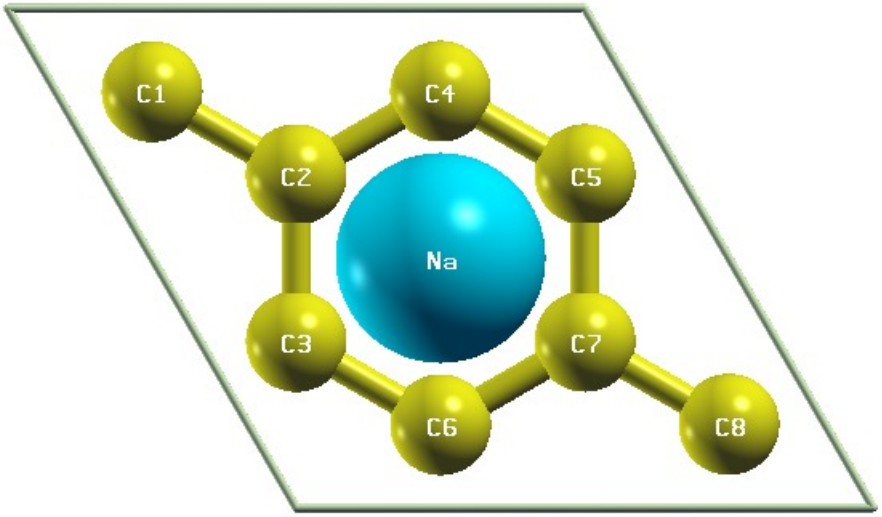


Figure 5.12: The sodium atom on the center of carbon ring within the hexagonal supercell.

### 5.4.2 Calculation in 3×3 supercell

3×3 supercell is the repetition of unitcell three times along X-direction and Y-direction as shown in Figure [5.13]. It has 18 number of carbon atoms.

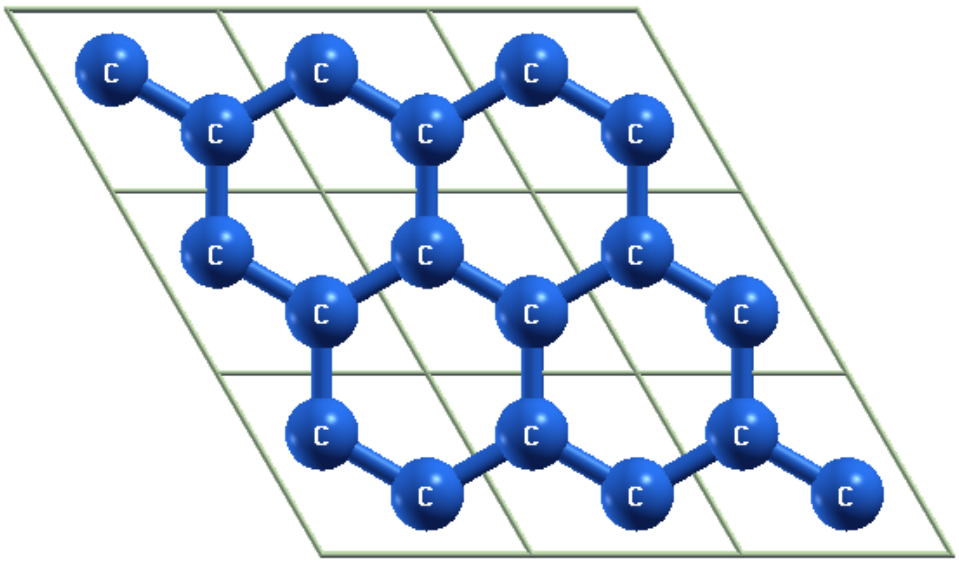


Figure 5.13: There are three unit-cells along X direction and three unit-cells along Y direction.

We have investigated the adsorption energy of the sodium atom on the three different sites: H, B, and T of the $3 \times 3$ supercell of graphene sheet. For this study sodium atom were kept at the distance of 2.33 Å, 2.42 Å, and 2.39 Å at sites H, B, and T respectively. The structure that we have used for the calculations are shown in Figure [5.14, 5.15, 5.16].

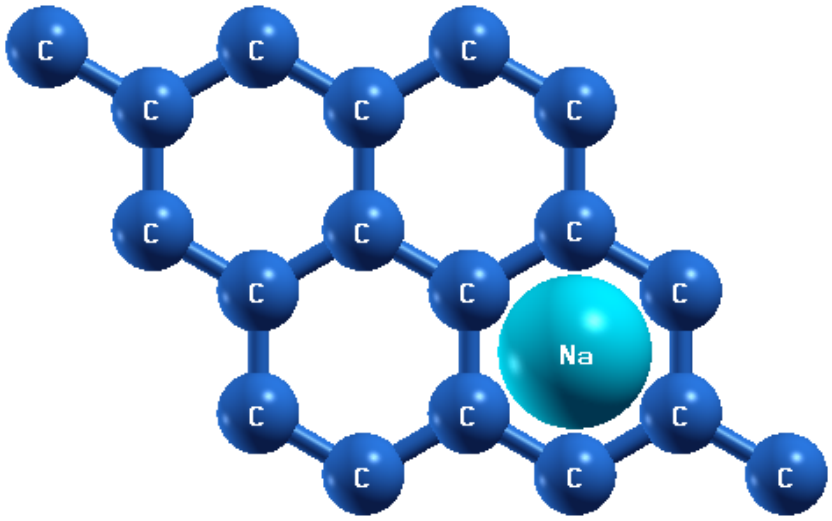


Figure 5.14: The input structure of sodium atom at the hollow site at the center of a hexagon above 2.33 Å from graphene sheet.

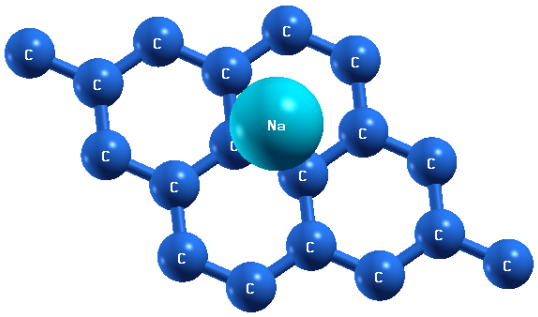


Figure 5.15: The input structure of sodium atom at the bridge site above 2.42 Åfrom graphene sheet.

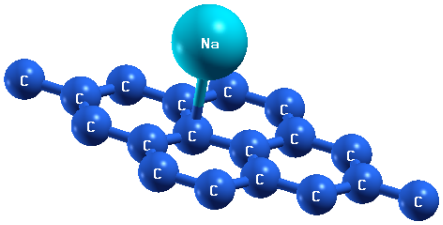


Figure 5.16: The input structure of sodium atom at the top site above a carbon atom 2.39 Åfrom graphene sheet.

We have performed the relax calculations under DFT-D2 level of approximation. From our investigations, we have found that the ground state energies of Na-graphene system are -297.419 Ry, -297.409 Ry, and -297.410 Ry for the sodium

atom in the H, B, and T sites of graphene respectively. The ground state energy of an isolated Na atom is -92.207 Ry and the ground state energy of pure graphene is -205.179 Ry. The adsorption energy of sodium atom in the sodium-graphene system is computed by using formula [5.3].

In case of $3 \times 3$ supercell, there are two possible configurations for the adsorption of sodium atom on graphene sheet at hollow position, see Figure [5.17, 5.18].

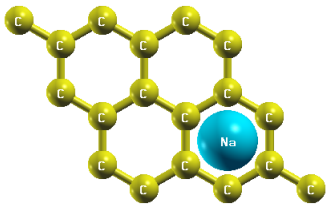


Figure 5.17: Sodium atom at the hollow position

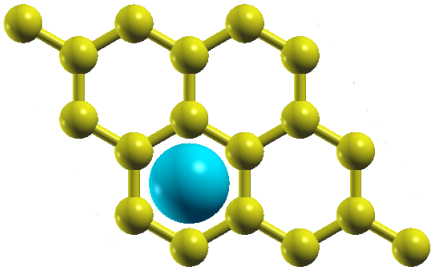

Figure 5.18: Sodium atom at the hollow position

We have calculated the adsorption energy for these two configurations. From our calculations, we have found that the adsorption energy of sodium atom is greater for the structure represented by Figure [5.17] (i.e 0.45 eV) than in Figure [5.18] (i.e 0.44 eV). Therefore, we have selected the structure represented in Figure [5.17] for our calculations.

We have presented the values of the adsorption energy, the equilibrium distances of the adatom (adatom height (h)), the distance between the sodium atom and nearest carbon atom ($d_{AC}$) of graphene and the distortion of graphene sheet in the Table [5.3].

Table 5.3: The property listed in the table are the adsorption energy of sodium atom $\Delta$E, height of the sodium atom from graphene sheet (h), nearest distance between the carbon atom of the sheet and sodium atom ($d_{AC}$), and the distortion observed on the sheet due to adsorption of sodium atom ($d_{GC}$).

| Atom | site | $\Delta$E (eV) | h (Å) | $d_{AC}$ (Å) | $d_{GC}$ ($10^{-2}$ Å) |
|---|---|---|---|---|---|
| Na | H | 0.45 | 2.32 | 2.72 | 0.94 |
| | B | 0.31 | 2.42 | 2.57 | -0.08 |
| | T | 0.33 | 2.41 | 2.48 | -0.53 |

From Table [5.3] it is seen that the adsorption energies or binding energies of sodium atom are 0.45 eV, 0.31 eV, and 0.33 eV at the hollow (H), bridge (H), and top (T) sites respectively. The positive values of binding energies signifies that the sodium atom bound to the graphene sheet. Of the three adsorption sites considered, the site with the large adsorption energy (minimum total energy) is referred to as the favored site. The equilibrium distance of sodium atom from the surface of graphene sheet are 2.32 Å for H site, 2.42 Å for bridge site, and 2.41 Åfor top site. The equilibrium distance is small for H site than for B and T sites which signifies that there exist strong interaction between sodium atom and carbon atoms at H site than at B and T sites. The adsorption energy is large and equilibrium distance of sodium atom from graphene sheet is minimum at the hollow site. Therefore, the hollow site is favorable for the adsorption of sodium atom in the graphene sheet, which agrees with previously reported results [2, 10, 27, 38]. For the bridge site and top site, the adsorption energy and equilibrium distance is almost same [27]. Similarly, the distance of the sodium atom from its nearest carbon atom $d_{AC}$ and for H, B, and T sites the values are 2.72 Å, 2.57 Å, and 2.48 Årespectively.

From Table [5.3], The distortion produced by sodium atom is only about 0.009 Å for hollow (H) site. This distortion is not significant (noticeable distortion is if $\geq$0.07 Å [27]). Also the distortion produced due to adsorption of sodium atom on the bridge and top sites is insignificant. Since the distortion in geometry of graphene sheet ($3 \times 3$ supercell) is not significant, C$-$C bonds near the adatom retain their $sp^2$ character and do not rehybridize significantly with any adatom orbitals.

The bond length (C-C), bond angle (C-C-C), and dihedral angle (C-C-C-C) in case

of pure graphene are 120.00$^o$, 1.42 Å, and 0.00$^o$ respectively. Which means that the carbon atoms in pure graphene sheet are in same plane. when sodium atom adsorbed on the graphene sheet the whole structure deformed. We have measured the structure changed by measuring bond lengths (Table [5.4]), bond angles (Table [5.5]) and change of dihedral angles (Table [5.6]).

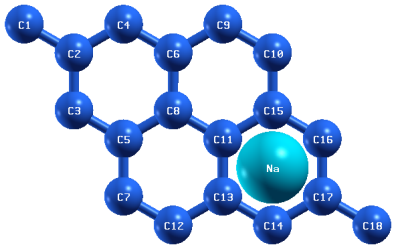


Figure 5.19: 3×3 supercell of graphene with 18 carbon atoms and one sodium atom at the hollow site.

The optimized geometry of Na-graphene system is represented by Figure [5.19]. From Figure [5.19], the adsorbed Na atom is in the hollow position of the hexagonal ring, formed by the carbon atoms (C11-C15-C16-C17-C14-C13-C11). The calculated values of bond length between various carbon atoms are presented in the Table [5.4].

Table 5.4: Bond length between the carbon-carbon atoms of the relaxed Na-graphene sheet.

| Bond between atoms | Na-graphene (Å) | pure graphene (Å) |
|---|---|---|
| (C1-C2), (C5-C7), (C6-C9) (C12-C13), (C8-C11), (C10-C15) (C2-C3), (C2-C4),(C17-C18) (C4-C6), (C6-C8), (C8-C5) (C5-C3), (C7-C12), (C9-C10) | 1.42 | 1.42 |
| (C11-C13), (C11-C15) (C16-C17), (C15-C16) (C17-C14) | 1.43 | 1.42 |

The Table [5.4] shows that the C-C bonds in the hexagonal ring (C11-C15, C15-C16, C16-C17, C17-C14, C14-C13, C13-C11), at which sodium atom adsorbed, are increased slightly due to adsorption. All other bonds (C1-C2, C5-C7, C6-C9, C12-C13, C8-C11, C10-C15, C17-C18, C2-C3, C2-C4, C4-C6, C6-C8, C8-C5, C5-C3, C7-C12, C9-C10) do not change.

Also the values of the bond angles of optimized structure, Figure [5.19], is presented in the Table [5.5]. The bond angle between the carbon atoms of pure graphene sheet is $120.00^o$. But due to the adsorption of sodium atom at hollow site of pure graphene, some change in the bond angle is observed.

Table 5.5: This table presents the bond angles of the relaxed geometry.

.

| Bond angle | for Na-graphene ($\theta^o$) | for pure graphene ($\theta^o$) |
|---|---|---|
| (C4-C2-C3), (C3-C5-C8), (C8-C6-C4) | $119.77^o$ | $120.00^o$ |
| (C2-C3-C5), (C5-C8-C6), (C6-C4-C2) | $120.23^o$ | $120.00^o$ |
| (C8-C5-C7), (C5-C7-C12), (C10-C9-C6), (C9-C6-C8), (C1-C2-C3), (C1-C2-C4), (C3-C5-C7), (C9-C6-C4) | $120.11^o$ | $120.00^o$ |
| (C7-C12-C13), (C11-C8-C5), (C15-C10-C9), (C6-C8-C11) | $119.89^o$ | $120.00^o$ |
| (C12-C13-C11), (C13-C11-C8), (C8-C11-C15), (C11-C15-C10), (C11-C13-C14), (C13-C14-C17), (C14-C17-C16), (C17-C16-C15), (C16-C15-C11), (C15-C11-C13), (C12-C13-C14), (C14-C17-C18), (C18-C17-C16), (C16-C15-C10) | $120.00^o$ | $120.00^o$ |

From Table [5.5], the maximum change in bond angle is about $0.23^o$ for (C4-C2-C3), (C3-C5-C8), (C8-C6-C4), (C2-C3-C5), (C5-C8-C6), (C6-C4-C2). Similarly, the bond angles (C8-C5-C7), (C5-C7-C12), (C10-C9-C6), (C9-C6-C8), (C1-C2-C3), (C1-C2-C4), (C3-C5-C7), (C9-C6-C4), (C7-C12-C13), (C11-C8-C5), (C15-C10-C9), (C6-C8-C11) are changed by $0.11^o$. Bond angles (C12-C13-C11), (C13-C11-C8), (C8-C11-C15), (C11-C15-C10), (C11-C13-C14), (C13-C14-C17), (C14-C17-C16), (C17-C16-C15), (C16-C15-C11), (C15-C11-C13), (C12-C13-C14), (C14-C17-C18), (C18-C17-C16), (C16-C15-C10) do not change.

The distortion of the 3×3 supercell of graphene sheet due to the adsorption of a sodium atom is calculated in terms of dihedral angles. The dihedral angles of pure graphene sheet is $0.00^o$ which means that all carbon atoms in pure graphene are in the same plane. When sodium atom adsorbed on the graphene sheet the dihedral angles changed. The change in dihedral angles are presented in Table [5.6].

Table 5.6: The changed in dihedral angles ($\triangle\phi^o$) when sodium atom adsorbed on the graphene sheet at hollow site.

.

| Dihedral angle | for Na-graphene | for pure graphene |
|---|---|---|
| (C1-C2-C4-C6), (C1-C2-C3-C5), (C2-C3-C5-C7), (C2-C4-C6-C9),(C9-C10-C15-C16), (C7-C12-C13-C14) | -0.03$^o$ | 0.00$^o$ |
| (C3-C5-C7-C12), (C4-C6-C9-C10) | -0.07$^o$ | 0.00$^o$ |
| (C2-C3-C5-C8), (C3-C5-C8-C6), (C5-C8-C6-C4), (C8-C6-C4-C2), (C6-C4-C2-C3), (C4-C2-C3-C5), | 0.10$^o$ | 0.00$^o$ |
| (C8-C5-C7-C12),(C15-C11-C13-C14),(C11-C13-C14-C17), (C13-C14-C17-C16), (C14-C17-C16-C15),(C17-C16-C15-C11), (C16-C15-C11-C13), (C12-C13-C11-C8), (C8-C11-C15-C10), (C10-C9-C6-C8) | 0.00$^o$ | 0.00$^o$ |
| (C5-C7-C12-C13), (C11-C8-C5-C7), (C15-C10-C9-C6), (C9-C6-C8-C11), (C6-C9-C10-C15) | 0.34$^o$ | 0.00$^o$ |
| (C7-C12-C13-C11), (C13-C11-C8-C5), (C11-C15-C10-C9), (C6-C8-C11-C15) | 0.34$^o$ | 0.00$^o$ |
| (C10-C15-C16-C17), (C15-C16-C17-C18), (C13-C14-C17-C18), (C12-C13-C14-C17) | -0.31$^o$ | 0.00$^o$ |

From Table [5.6], the maximum change in dihedral angles is about 0.34$^o$ for (C5-C7-C12-C13), (C11-C8-C5-C7), (C15-C10-C9-C6), (C9-C6-C8-C11), (C6-C9-C10-C15), (C7-C12-C13-C11), (C13-C11-C8-C5), (C11-C15-C10-C9). Similarly, the dihedral angles (C8-C5-C7-C12),(C15-C11-C13-C14),(C11-C13-C14-C17), (C13-C14-C17-C16), (C14-C17-C16-C15),(C17-C16-C15-C11), (C16-C15-C11-C13), (C12-C13-C11-C8), (C8-C11-C15-C10), (C10-C9-C6-C8), do not change, which signifies that there is no effects of adsorption of sodium.

Table [5.2] and Table [5.3], from the values of adsorption energies it is seen that the sodium atom is not bound to $2 \times 2$ supercell of the graphene (having 8 carbon atoms) whereas it is bound to $3 \times 3$ supercell of graphene (having 18 carbon atoms). Also, sodium atom stays close to the graphene sheet in case of $3 \times 3$ supercell than it does in $2 \times 2$ supercell of graphene because equilibrium distances of sodium atom are small in $3 \times 3$ than in $2 \times 2$ supercell of graphene.

### 5.4.3 Calculation in 4×4 supercell

4×4 supercell, containing 32 number of carbon atoms, is the repetition of unitcell four times along X-direction and Y-direction as shown in Figure [5.20].

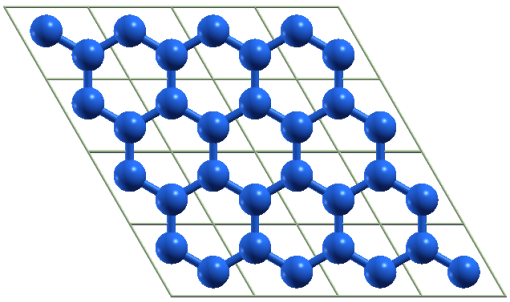

Figure 5.20: There are four unit-cells along X direction and four unit-cells along Y direction.

The most favorable site for adsorption of sodium atom in the graphene sheet is hollow site. Therefore, in case of 4×4 supercell of graphene we have performed the relax calculations only for hollow site. The calculations carried out under DFT-D2 level of approximation.

In our calculations, we kept the sodium atom at the hollow position at distance 2.69 Å above from each of carbon atom of hexagonal ring. We have performed the relax calculations under DFT-D2 level of approximation. From our calculations, we have found the ground state energies of pure graphene sheet, isolated sodium atom, and sodium adatom graphene system are -364.768 Ry, -92.192 Ry, and -457.017 Ry respectively. The ground state energies are calculated using the same dimension of supercell i.e. $4 \times 4$ supercell. The adsorption energy of sodium atom in the sodium-graphene system is computed by using Formula [5.3]. The adsorption energy or binding energy of sodium atom is 0.78 eV. Similarly, the equilibrium distance between the sodium atom and graphene sheet is 2.25 Å, which agrees with previous result [27]. Also, the distance of nearest carbon atom from sodium atom is

2.69 Å. From these calculations, we found that the sodium atom strongly bound and stay close to the graphene sheet in 4×4 supercell than in 3×3 supercell (Table [5.3]).

In the case of 4×4 supercell, the distortion produced by sodium atom to the graphene sheet is insignificant. The distortion is about 0.008 Å, which is small than the distortion produce in 3×3 supercell of graphene i.e 0.009 Å. The small positive distortion implies that there is small movement of graphene sheet towards the sodium atom.

The optimized geometry of sodium-graphene system represented by Figure [5.21].

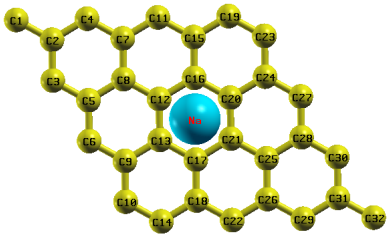


Figure 5.21: The optimized geometry of the sodium-graphene system.

From figure [5.21], the adsorbed Na atom is in the hollow position of the hexagonal ring formed by the carbon atoms (C12, C13, C17, C21, C20, and C16). In case of pure graphene sheet, the bond length (C-C), bond angle (C-C-C), and dihedral angle (C-C-C-C) are 1.42 Å, 120.00$^o$, and 0.00$^o$ respectively but when sodium atom adsorbed on the graphene sheet the whole structure changed. We have measured the structure changed in terms of bond lengths (Table [5.7]), bond angles (Table [5.8]), and dihedral angles (Table [5.9]).

The bond lengths between various carbon atoms are presented in Table [5.7].

Table 5.7: Bond lengths between carbon atoms in the optimized geometry of Na-graphene system.

.

| Bond length between atoms | for Na-graphene (Å) | for pure graphene (Å) |
|---|---|---|
| (C1-C2), (C2-C3), (C3-C5), (C2-C4),(C30-C31), (C31-C32) (C4-C7), (C26-C29), (C28-C30), (C7-C8), (C5-C8), (C28-C25), (C25-C26), (C11-C15), (C6-C9), (C27-C24), (C18-C22), (C14-C18) (C9-C10), (C15-C19), (C23-C24), (C7-C11), (C5-C6), (C28-C27), (C22-C26), (C10-C14), (C19-C23), (C15-C16), (C8-C12), (C9-C13), (C24-C20), (C21-C25), (C17-C18) | 1.42 | 1.42 |
| (C16-C12), (C13-C12), (C20-C21) (C21-C17), (C13-C17), (C16-C20) | 1.43 | 1.42 |

From the table [5.7], bond lengths of the carbons atoms, (C16-C12), (C13-C12), (C20-C21),(C21-C17), (C13-C17), (C16-C20), of the hexagonal ring, above which sodium atom adsorbed, are increased. The bond lengths for (C3-C5), (C4-C7), (C26-C29), (C28-C30), (C7-C8), (C5-C8), (C28-C25), (C25-C26), (C11-C15), (C6-C9), (C27-C24), (C18-C22), (C14-C18), (C9-C10), (C15-C19), (C23-C24), (C7-C11), (C5-C6), (C28-C27), (C22-C26), (C10-C14), (C19-C23), (C15-C16), (C8-C12), (C9-C13), (C24-C20), (C21-C25), (C17-C18), (C1-C2), (C2-C3), (C2-C4), (C30-C31), and (C31-C32) do not change.

We have also studied about the bond angles which is presented in Table [5.8].

Table 5.8: The bond angles ($\theta^o$) of carbon atoms in the optimized geometry of 4×4 supercell.

.

| Bond angle | for Na-graphene ($\theta^o$) | for pure graphene ($\theta^o$) |
|---|---|---|
| (C1-C2-C3), (C1-C2-C4), (C16-C12-C13), (C12-C13-C17), (C13-C17-C21), (C17-C21-C20), (C21-C20-C16), (C20-C16-C12), (C29-C31-C30), (C30-C31-C32), (C29-C31-C32) | $120.00^o$ | $120.00^o$ |
| (C2-C4-C7), (C5-C3-C2), (C26-C29-C31), (C31-C30-C28), (C29-C26-C22), (C6-C5-C3), (C4-C7-C11), (C27-C28-C30) | $120.08^o$ | $120.00^o$ |
| (C4-C7-C8), (C25-C26-C29) (C8-C5-C3), (C30-C28-C25) | $119.78^o$ | $120.00^o$ |
| (C7-C8-C5), (C28-C25-C26), (C22-C18-C14), (C10-C9-C6), (C11-C15-C19), (C23-C24-C27) | $120.27^o$ | $120.00^o$ |
| (C11-C7-C8), (C15-C11-C7), (C8-C5-C6), (C5-C6-C9), (C24-C23-C19), (C23-C19-C15), (C9-C10-C14), (C10-C14-C18), (C25-C28-C27), (C28-C27-C24), (C18-C22-C26), (C22-C26-C25) | $120.14^o$ | $120.00^o$ |
| (C7-C8-C12), (C16-C15-C11), (C12-C8-C5), (C6-C9-C13), (C19-C15-C16), (C20-C24-C23), (C13-C9-C10), (C14-C18-C17), (C21-C25-C28), (C27-C24-C20), (C17-C18-C22), (C26-C25-C21), | $119.87^o$ | $120.00^o$ |
| (C8-C12-C16), (C12-C16-C15), (C9-C13-C12), (C13-C12-C8), (C15-C16-C20), (C16-C20-C24), (C18-C17-C13), (C17-C13-C9), (C24-C20-C21), (C20-C21-C25), (C21-C17-C18), (C25-C21-C17), | $119.99^o$ | $120.00^o$ |

Table [5.8] shows that the bond angles of the carbon atoms (C12-C13-C17-C21-C20-C16) of the hexagonal ring, above which sodium atom adsorbed, do not change. We have found that the maximum change of bond angles is $0.27^o$ for (C7-C8-C5), (C28-C25-C26), (C22-C18-C14), (C10-C9-C6), (C11-C15-C19), (C23-C24-C27).

The distortion of planner structure of the 4×4 supercell of graphene sheet due to the adsorption of a sodium atom is demonstrated by the observed values of the dihedral angles presented in Table [5.6]. The dihedral angles in case of the pure graphene is $0.00^o$ which implies that all carbon atoms are in the same plane.

Table 5.9: Change in dihedral angles ($\triangle\phi^o$) on optimized geometry of sodium adsorbed graphene system.

.

| Dihedral angles | for Na-graphene | for pure graphene |
|---|---|---|
| (C1-C2-C3-C5), (C26-C29-C31-C32), (C32-C31-C30-C28), (C7-C4-C2-C1), | -0.37$^o$ | 0.00$^o$ |
| (C2-C3-C5-C6), (C22-C26-C29-C31), (C31-C30-C28-C27), (C11-C7-C4-C2), | -0.03$^o$ | 0.00$^o$ |
| (C3-C5-C6-C9), (C30-C28-C27-C24), (C15-C11-C7-C4) | -0.18$^o$ | 0.00$^o$ |
| (C5-C6-C9-C10), (C6-C9-C10-C14), (C10-C14-C18-C22) (C14-C18-C22-C26), (C18-C22-C26-C29), (C28-C27-C24-C23), (C27-C24-C23-C19), (C23-C19-C15-C11), (C19-C15-C11-C7), | -0.53$^o$ | 0.00$^o$ |
| (C18-C22-C26-C25), (C25-C21-C17-C18), (C18-C17-C13-C9) (C24-C20-C21-C25), (C25-C28-C27-C24), (C9-C10-C14-C18), (C24-C23-C19-C15), (C8-C12-C16-C15), (C15-C11-C7-C8), (C8-C5-C6-C9), (C9-C13-C12-C8), (C8-C5-C6-C9), (C15-C16-C20-C24), (C24-C23-C19-C15), (C16-C12-C13-C17), (C12-C13-C17-C21), (C13-C17-C21-C20), (C17-C21-C20-C16), (C21-C20-C16-C12), (C20-C16-C12-C13), (C16-C12-C13-C17), | 0.00$^o$ | 0.00$^o$ |
| (C4-C7-C8-C5), (C7-C8-C5-C3), (C28-C25-C26-C29) (C30-C28-C25-C26), | 0.71$^o$ | 0.00$^o$ |
| (C5-C3-C2-C4), (C3-C2-C4-C7), (C26-C29-C31-C30), (C29-C31-C30-C28) | 0.28$^o$ | 0.00$^o$ |
| (C11-C7-C8-C12), (C16-C15-C11-C7), (C11-C7-C8-C12), (C5-C6-C9-C13), (C12-C8-C5-C6), (C20-C24-C23-C19), (C23-C19-C15-C16), (C13-C9-C10-C14), (C10-C14-C18-C17), (C28-C27-C24-C20), (C17-C18-C22-C26), (C22-C26-C25-C21), | 0.69$^o$ | 0.00$^o$ |
| (C7-C8-C12-C16), (C12-C16-C15-C11), (C6-C9-C13-C12), (C13-C12-C8-C5), (C16-C20-C24-C23), (C19-C15-C16-C20), (C14-C18-C17-C13), (C17-C13-C9-C10), (C20-C21-C25-C28), (C21-C25-C28-C27), (C27-C24-C20-C21), (C21-C17-C18-C22), (C26-C25-C21-C17), | 0.69$^o$ | 0.00$^o$ |
| (C2-C4-C7-C8), (C8-C5-C3-C2), (C2-C4-C7-C8), (C25-C26-C29-C31), (C31-C30-C28-C25), | 0.21$^o$ | 0.00$^o$ |

From Table [5.6], the maximum change in the dihedral angle is 0.71$^o$ for (C4-C7-C8-C5), (C7-C8-C5-C3), (C28-C25-C26-C29), and (C30-C28-C25-C26). The change in dihedral angles for others vary in between 0.00$^o$ to 0.71$^o$. Some dihedral angles do not vary which indicates that there is no effects of adsorption of sodium atom. Similarly, the change of dihedral angles small means the distortion produced by adatom to the graphene sheet is small.

From our calculations, we have found that the adsorption energies of sodium atom are -0.29 eV, 0.45 eV, and 0.78 eV for the graphene sheet having 8 ($2 \times 2$ supercell), 18 ($3 \times 3$ supercell) and 32 ($4 \times 4$ supercell) number of carbon atoms respectively. The adsorption energy (binding energy) of the sodium atom increases when the number of carbon atoms in the graphene sheet increases, see Figure [5.22].

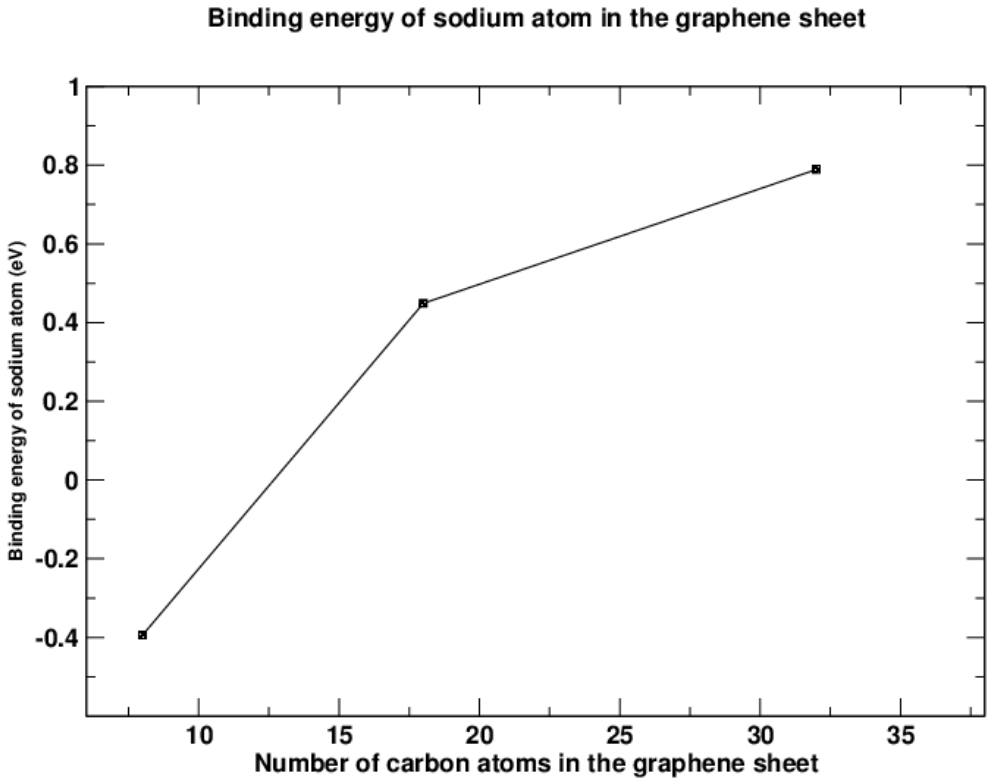


Figure 5.22: The graph is the variation of the adsorption energy of sodium atom when the number of the carbon atoms in the graphene sheet increases.

From Figure [5.22], the binding energy of sodium atom up to 18 number of carbon atoms in the graphene sheet increases almost linearly. When number of carbon atoms increases beyond 18, binding energy of sodium atom still increases but less rapidly.

## 5.5 Charge transfer

Charge transfer is an ambiguous quantity and there is no unique definition of charge transfer. The study of charge transfer is important to discuss the bonding of adatom and the graphene. Charge transfer is the most sensible in the context of ionic bonding. In case of covalent bonding, charge is shared in the bond between adsorbate and substrate. In such case charge transfer becomes less relevant [27].

There are many ways to calculate the charge transfer in alkali metal adsorption in graphene [40, 41, 42, 43]. In our calculations, we have used the method of charge density difference. According to this method, the charge-density difference is defined as

$$\triangle\rho(\mathbf{r}) = \rho_{G+Na}(\mathbf{r}) - \rho_{Na}(\mathbf{r}) - \rho_{G}^{relaxed}(\mathbf{r}) \tag{5.4}$$

The quantity $\rho_{G+Na}$ is the charge density of the sodium-graphene system. The charge density of the isolated sodium atom (without graphene) in the 3×3 supercell is $\rho_{Na}$ and it is calculated by removing the graphene sheet from optimized structure of the sodium-graphene system. The quantity $\rho_G$ is the charge density of an isolated 3×3 graphene layer, it is calculated by removing the adatom from optimized structure of the sodium-graphene system. This structure is different than the optimized structure of the pure graphene. The charge-density difference, quantifies the redistribution of electron charge due to the adatom-graphene interaction. All the quantities in Equation [5.4] are computed in the same size of the hexagonal supercell.

To calculate the charge density difference as given by equation [5.4], we have prepared an input file 'avg.in'. Then by using an executable 'average.x', we have calculated charge density difference. The output of 'avg.in' contains charge density difference as a function of Z coordinate along the height of supercell. In order to calculate the charge transfer, we have multiplied the charge density difference by the area of the supercell to give the linear charge density difference as a function of position. Figure [5.23] shows the variation of the linear charge-density as a function of distance of sodium atom at hollow site.

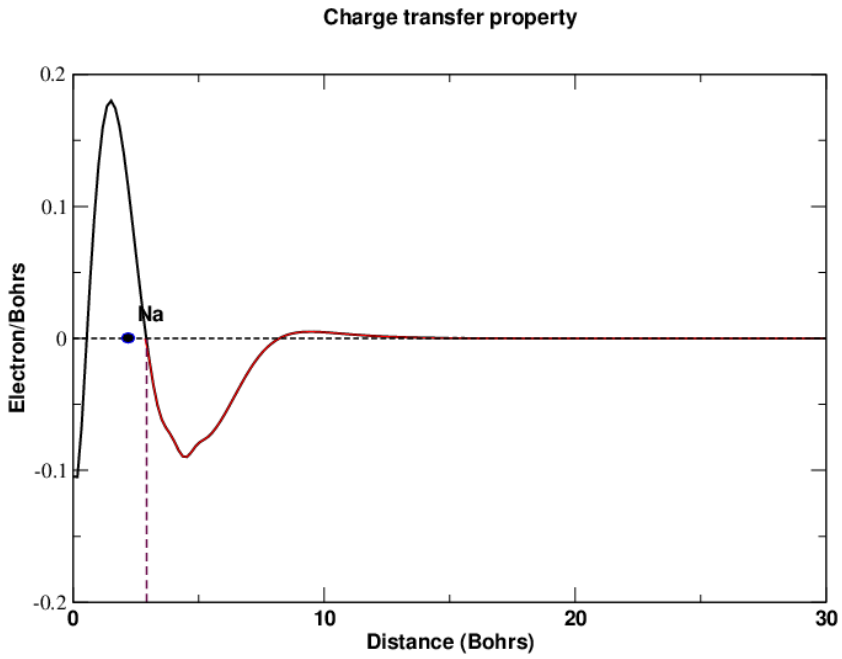


Figure 5.23: The variation of the linear charge-density (electrons/Bohr) as a function of the distance of sodium on the hollow site. The position of the graphene sheet at z = 0 and sodium atom is at z = 2.92 Bohrs indicated by vertical line. The vertical line z = 2.92 Bohrs indicates $R_{cut}$. The integration between the region z = 0 and z = 2.92 Bohrs gives total charge transfer.

In the Figure [5.23], the region near the graphene sheet is named as substrate (z≤2.92 Bohrs) and the region above the adatom is named as adsorbate (z≥2.92 Bohrs). The line with z = 2.92 Bohrs represent the ($R_{cut}$) cutoff distance. An adsorbate-substrate cutoff distance $R_{cut}$ is defined as the distance from the graphene plane to the point between the plane and the adatom at which charge accumulation changes to charge depletion for charge transfer from the adatom to the graphene.

The amount of charge transfer due to adsorption of sodium atom on hollow site of graphene are 0.09 e, 0.21 e, and 0.30 e respectively for $2 \times 2$, 3×3, and 4×4 supercell of graphene.

## 5.6 Band structure

The atom in a solid are closely packed. When the atoms are brought together in a solid, the interaction between them perturbs the initial atomic levels. Most of

the symmetry of the electronic states in the isolated atom is deformed and the level splits into bands of levels. A band constitutes a sort of energy continuum, in which separate levels due to individual atoms cannot be identified. In the process of inter atomic interaction, the inner shell electron states are the least effected, whereas the valence electrons, which are closest to neighboring ions, are the most effected. The effect of bringing one atom closer to the other is to split a single sharp energy level into pair of levels [45].

In case of solids, the discrete energy levels of an isolated atom perturbed through quantum mechanical effects, and the electrons occupy a band of energy levels called the valence band. Empty states in each single atom also broaden into a band of energy levels that is normally empty, called the conduction band. Conduction band and valence band are the allowed regions for electrons to remain [46]. There are certain region in some solids like insulators and semiconductors for which no electronic orbitals exist. This region of energy is forbidden and called band gap. Band gaps are the consequence of the interaction of conduction electron waves with ion cores [47]. Just as electrons at one energy level in an individual atom may transfer to another empty energy level, electrons in the solid may transfer from one energy level in a given band to another energy level either of the same band or other band, often crossing an intervening gap of forbidden energies (band gap).

There are different methods available for the band structure calculations. We have used Quantum ESPRESSO-5.0.1 package [14], in the present work, to calculate the band structure of pure graphene and sodium adsorbed graphene system. Because of symmetry, we can obtain whole crystal from the first Brillouin zone. Hence, the solution of the entire solid can be characterized by their behavior in a single Brillouin zone. In the present work, we are concentrated only on the first Brillouin zone. The first Brillouin zone is the smallest volume enclosed by the planes that are perpendicular bisectors of the reciprocal lattice vectors drawn from the origin. The first Brillouin zone of the hexagonal lattice with high symmetric points: $\Gamma$, K, and M is shown Figure [5.24].

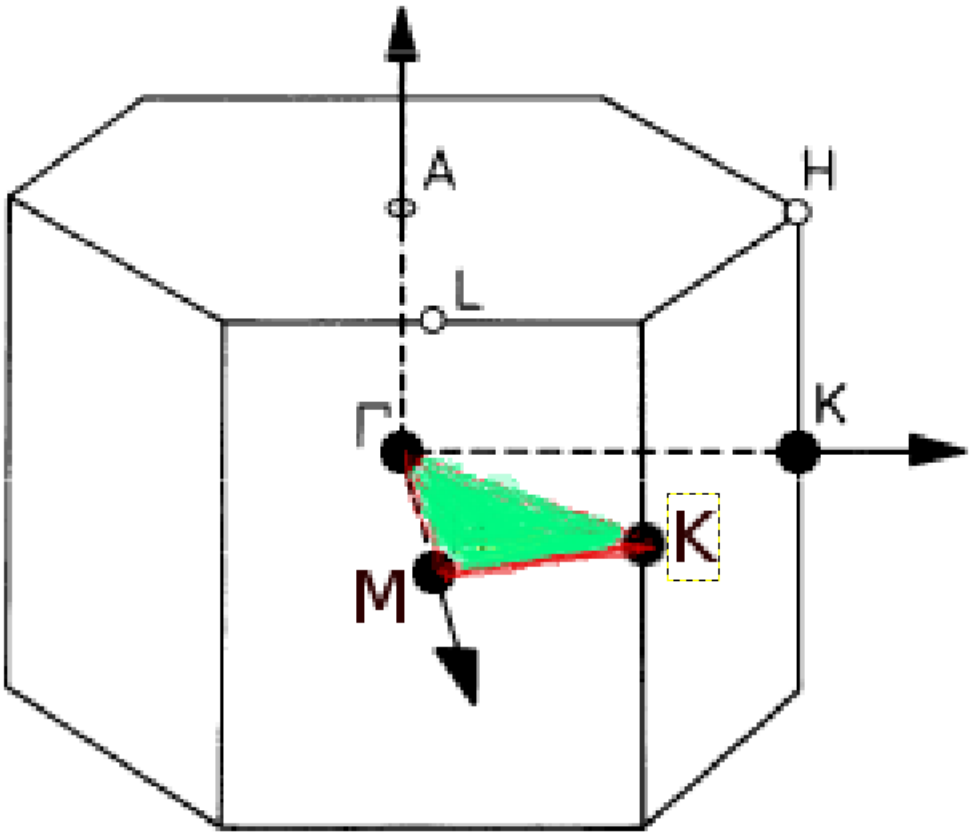


Figure 5.24: The first Brillouin zone of hexagonal and triangular part Γ-K-M represent the irreducible Brillouin zone.

### 5.6.1 Band structure of pure graphene

Figure [5.25], represent the band structure of pure graphene.

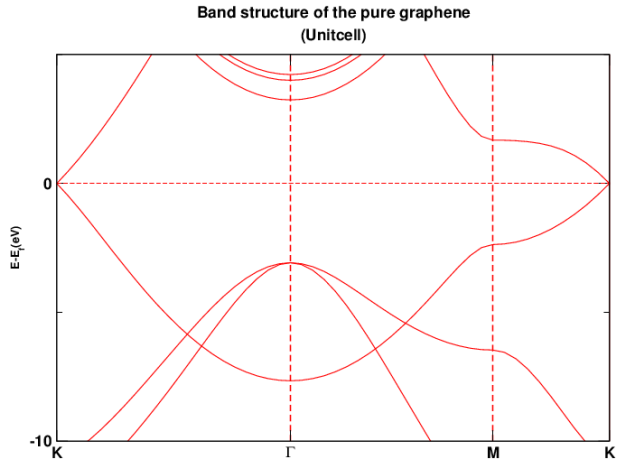


Figure 5.25: The band structure of the graphene with K-Γ-M-K irreducible Brillouin zone. The X-direction represents high symmetric points and Y-axis represents energy shifted from Fermi level.

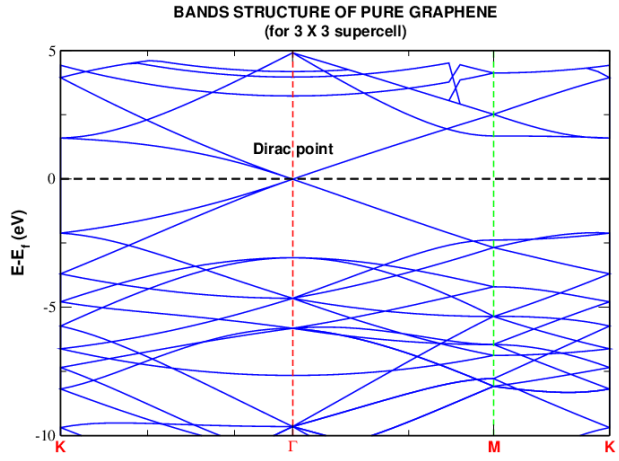


Figure 5.26: The band structure of the pure graphene .

We have performed the band structure calculations by defining the high symmetric points (i.e Γ, K, and M) on the edges of irreducible Brillouin zone , see Figure [5.24]. In our study, we have taken 100 k-points along the specific direction of irreducible Brillouin zone in order to obtain fine band structure. The band structures of pure graphene are shown in Figure [5.25] and Figure [5.26]. Figure [5.25], we have performed the band structure calculations along the path K-Γ-M-K in irreducible

Brillouin zone. Similarly, for Figure [5.26], we have performed the calculations along the path Γ-K-M-Γ in irreducible Brillouin zone.

Graphene is a single atomic layer of graphite where the carbon atoms condense in a honeycomb lattice due to their $sp^2$ hybridization of $2s$, $2p_x$, and $2p_y$ orbitals of three valence electrons out of four valence electrons. The mixing of the 2s and two 2p orbitals gives the planar $sp^2$ hybridization. The electrons which involve for $sp^2$ hybridization are localized and form $\sigma$ bond. These electrons do not contribute for the transport phenomenon. The fourth electron is perpendicular to the plane of graphene sheet occupies the $2p_z$ orbital and form the $\pi$-bond with $2p_z$ electron of neighboring carbon atom [4, 8]. The electrons which form $\pi$-bond are delocalized over the entire lattice and has higher energy than the electrons that form the $\sigma$-bonds. Most of the interesting property of the graphene arise due to this delocalized $\pi$-electron [32]. The band above the Fermi level refer to $\pi^*$ and below the Fermi level refer to $\pi$ band. Figure [5.26] shows that, in case of pure graphene band gap is zero form by the $\pi$ states of electron. The $\pi^*$ and $\pi$ bands meet at the Fermi level.

The $\pi$ states of electron form a band which have a conical self-crossing point at the high symmetry point, Figure [5.26]. The conical point is known as the Dirac point and the conical region around the Dirac point is known as Dirac cone. In case of pure graphene, the Dirac point exactly lies on the Fermi level. The Dirac point and Dirac cone can be seen in Figure [5.26]. The band above the Fermi level is conduction band which is empty and the band below the Fermi level is valence band which is occupied. The band gap of pure graphene is zero which indicates that, graphene is zero band gap semiconductor. The dispersion curve of pure graphene around the Dirac point is same as the dispersion curve of ultra-relativistic particles (Dirac particles) i.e particles obey the linear dispersion relations. Due to this reason, the effective mass of the electrons (Dirac particles) around this conical region or near Fermi level is zero and velocity is high enough. So, in case of pure graphene, the electronic transport properties is governed by the Dirac relativistic equations.

### 5.6.2 Band structure of sodium-graphene system

Figure [5.27], represent the band structure of sodium adatom graphene system.

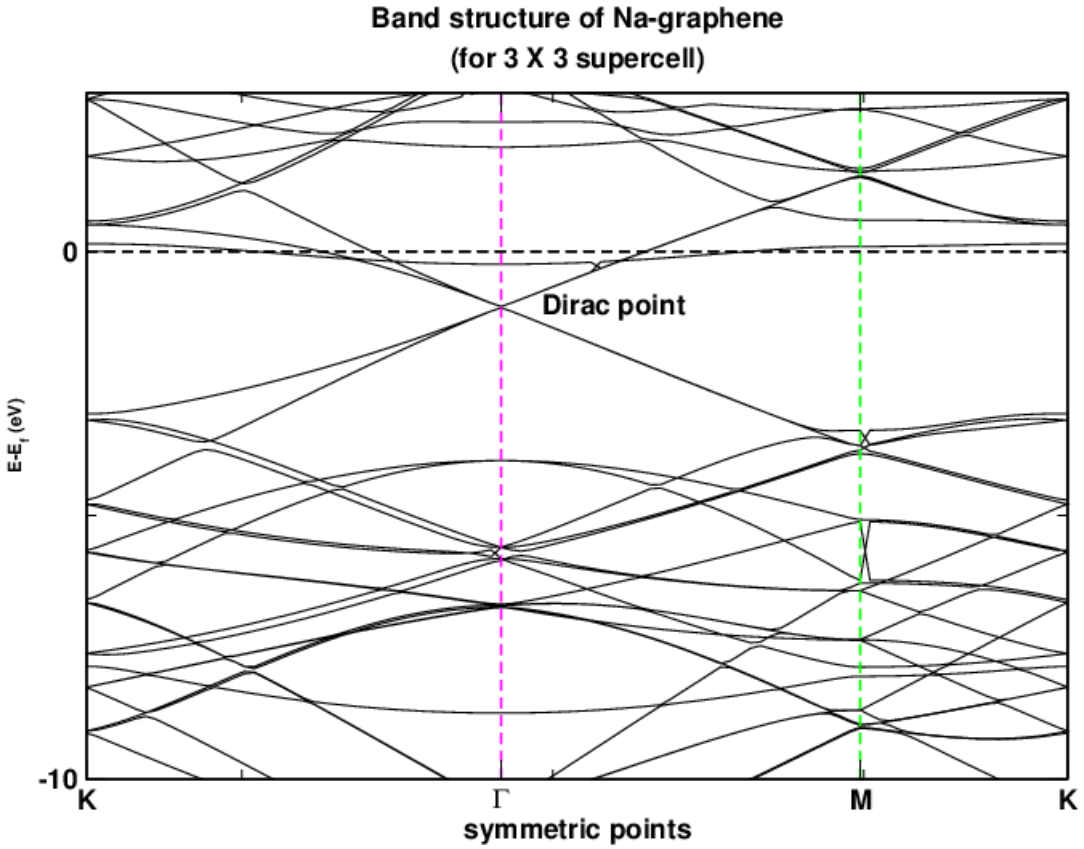


Figure 5.27: The bands structure of Na-graphene system in 3×3 supercell.

We have calculated the band structure of Na-graphene system. From Figure [5.27],the conical point (Dirac point) shifted below the Fermi level due to adsorption of sodium atom on a graphene . The conical point shifted 1.084 eV below the Fermi level. Before adsorption of sodium atom on the graphene, the $\pi$ and $\pi^*$ bands are just meet at the Fermi level. In this case, all the states of $\pi$ band are completely filled up and $\pi^*$ band are empty . When we adsorbed the Na atom on the graphene, some effective amount of charge transfer from sodium atom to the graphene occurred. The $\pi$ band of the graphene is already occupied so that the available charge from sodium atom occupied the $\pi^*$ band [28].

In case of pure graphene, the Fermi level is at -2.346 eV but when sodium atom adsorbed, the level raise to the value -0.695 eV. This means the Fermi level shifted 1.651 eV upward i.e. after adsorption of sodium atom Fermi level shifted towards

the conduction band. From our study, we found that the conduction band and valence band overlapped. The band structures of sodium-graphene system suggest that these materials can be use as conductors.

## 5.7 Density of states (DOS)

The density of states is defined as the number of orbitals per unit energy range provided that each energy level can be occupied by the particles. The density of states refers to the number of quantum states per unit energy range and it indicates how densely packed quantum states in a particular system. The study of density of states is important because from the density of states, we can predict about electronic and magnetic properties of the system such as specific heat, paramagnetic susceptibility, and other transport phenomena. Further, the density of states provides numerical information on the states availability at each energy level. A high value for the density of states represents a high number for the energetic states ready to be occupied. If there are no available states for occupation in an energetic level, the value for the density of states will be zero [45].

### 5.7.1 Density of states of pure graphene

Figure [5.28] represents the DOS of pure graphene system having the 18 carbon atoms.

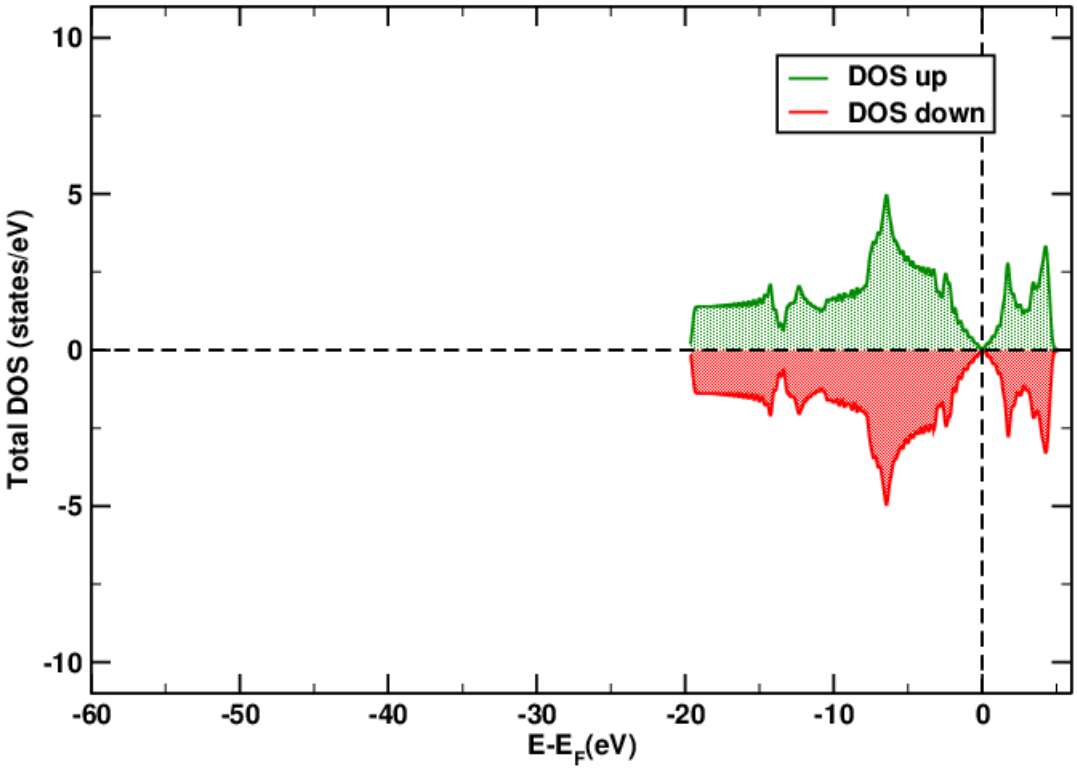


Figure 5.28: Density of states of pure graphene. The vertical dotted line represents Fermi level. Above the horizontal dotted line represents the DOS for spin up and below this line represents DOS for spin down.

In the Figure [5.28], we have plotted the DOS for spin up and spin down states on the reference of Fermi level. The Fermi level is represented by vertical dotted line. In case of pure graphene, the Fermi level lies at -2.35 eV. This figure clearly shows that the DOS for spin up and spin down is symmetrical. Dirac point where DOS is zero, exactly lies at the Fermi level. Due to symmetrical nature of up and down DOS, the pure graphene shows non-magnetic behavior.

### 5.7.2 Density of States of Na adsorbed graphene

Figure [5.29] represent the DOS of sodium adsorbed graphene system.

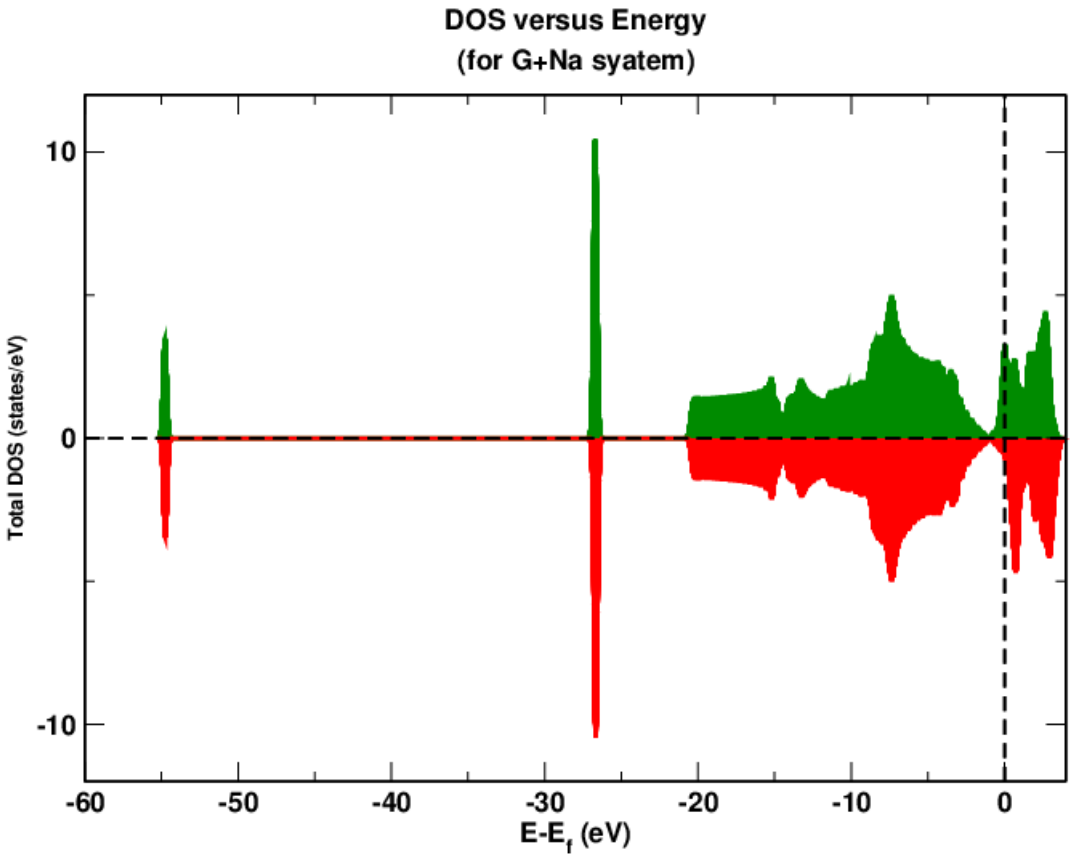


Figure 5.29: The plot between density of states versus energy .

In the Figure [5.29], the vertical dotted line represents the Fermi level. From Figure [5.29], the Dirac point where DOS is zero, shifted below the Fermi level in case of sodium-graphene system. The whole structure is not symmetrical. This signifies that the Na-graphene system is magnetic. In case of 3×3 supercell of graphene, the value of magnetization is 0.08 $\mu_B$ and in case of 4×4 supercell of graphene, the value of magnetization is 0.24 $\mu_B$. In case of 4×4 supercell our calculated value agrees with previously reported value 0.27 $\mu_B$ [27]. The adsorption of Na on the graphene leads to net magnetization (0.24 $\mu_B$) that is reduced from that of isolated sodium atom (1.0 $\mu_B$ ). This reduction in magnetization is due to the partial charge transfer from isolated sodium atom to the graphene.

The DOS of sodium decorated graphene system, see Figure [5.29], is different than the DOS of pure graphene system, see Figure [5.28], i.e the DOS of sodium-graphene system has been modified. The modification occurs near the Fermi level and at -26.69 eV, -54.77 eV . These modification is due to the contribution from different

orbitals of the sodium atom, Figure [5.30,5.31].

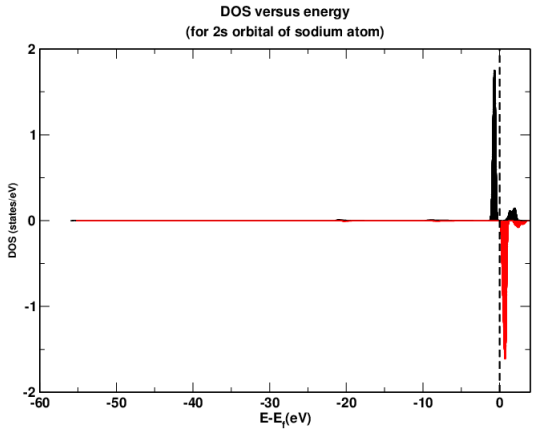


Figure 5.30: Projected density of states (PDOS) for spin up and spin down of 2s orbitals of sodium atom.

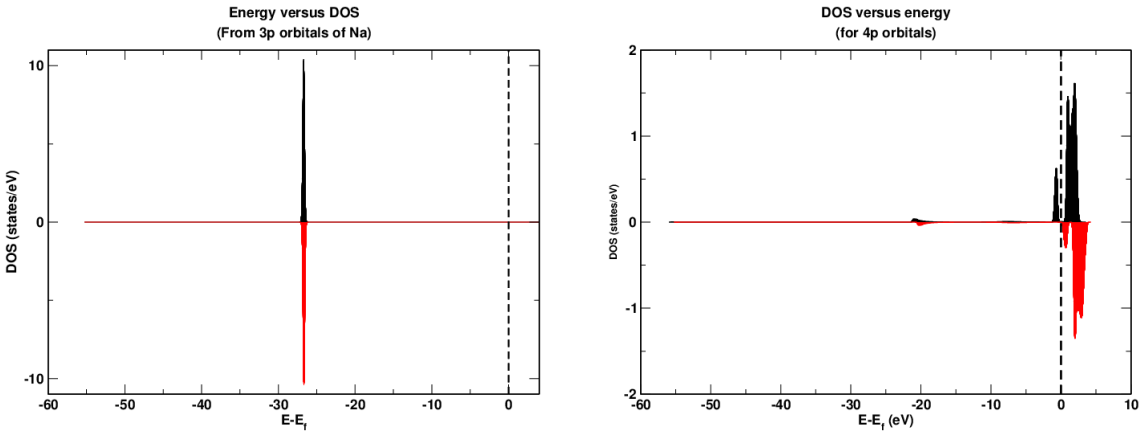


Figure 5.31: Projected density of states (PDOS) for spin up and spin down of 3p and 4p orbitals of sodium atom .

Figure [5.30, 5.31], shows that the modification of DOS of sodium-graphene system is due to the 2s, 3p, and 4p orbitals of the sodium atom. The change of DOS of Na-graphene at around -26.69 eV is due to the contribution of $3p$ orbitals of sodium atom. There is also modification occur in the DOS of Na-graphene system near the Fermi level. $2s$ and $4p$ orbitals of sodium atom play the main role for this modification.

The DOS of the sodium-graphene system also indicate that these materials can be use as conductors [28].

## 5.8 Adsorption of hydrogen molecules on the Na-graphene

We have investigated the stability of the hydrogen adsorption on the sodium decorated graphene system. Before performing the adsorption of $H_2$ molecule on Na-graphene system, the bond length between the hydrogen atoms of a $H_2$ molecule is needed. To calculate the bond length, we have taken a $H_2$ molecule in the 3×3 supercell of graphene and performed the relax calculations. We have found the bond length 0.75 Å which agrees with the experimental value [44]. Due to the periodicity of the crystal, when $H_2$ molecule taken in the volume of 3×3 supercell of graphene, it see the another $H_2$ molecule at the distance equal to the cell dimension (i.e. at 9.299 Bohrs). This distance is large compared to the bond length (i.e. 1.418 Bohrs) and hence there is no interaction between two hydrogen molecules separated by that distance.

We have studied the interaction between the pure graphene sheet and single hydrogen molecule. For this calculation, we have taken the graphene sheet having 18 carbon atoms and the single molecule of hydrogen at different positions:

• The $H_2$ molecule perpendicular to the carbon atom, see Figure [5.32].

• The $H_2$ molecule perpendicular to the midpoint of carbon-carbon bond, see Figure [5.33].

• The $H_2$ molecule perpendicular to the center of a hexagonal ring, see Figure [5.34].

• The $H_2$ molecule horizontal on the hexagonal ring, see Figure [5.35].

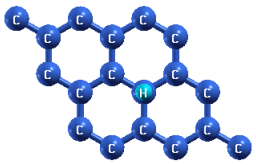

Figure 5.32: $H_2$ molecule perpendicular to the carbon atom.

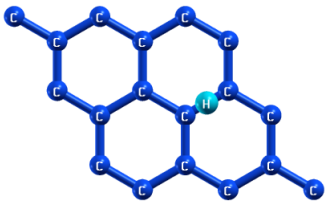

Figure 5.33: $H_2$ molecule perpendicular to the carbon-carbon bond.

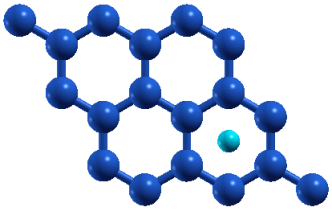

Figure 5.34: $H_2$ molecule perpendicular to the center of hexagonal ring.

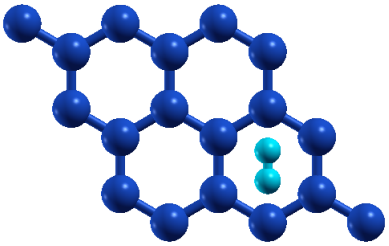

Figure 5.35: $H_2$ molecule horizontal to the hexagonal ring .

We have obtained the binding energy and equilibrium position of the $H_2$ molecule from optimized geometry of $H_2$-graphene system. The binding energy ($\Delta E$) of the $H_2$ molecule is calculated as

$$E = E_{G+H_2} - E_G - E_{H_2} \tag{5.5}$$

where $E_G$, $E_{H_2}$, and $E_{G+H_2}$ is the ground state energy of pure graphene, hydrogen molecule, and $H_2$-graphene system. These parameters are calculated using same size of the supercell of graphene. The binding energy of $H_2$ molecule and distance of molecule from the graphene plane are presented in Table [5.10].

Table 5.10: Binding energy of $H_2$ on the different sites of the graphene and equilibrium distance of $H_2$ molecule from graphene sheet.

| Position of $H_2$ molecule | Binding energy $\Delta$E (meV) | distance of $H_2$ from graphene sheet ($\mathring{A}$) |
|---|---|---|
| perpendicular on bridge | 62.9 | 2.67 |
| perpendicular above carbon atom | 61.9 | 2.72 |
| perpendicular on hexagon | 68.6 | 2.48 |
| horizontal on hexagon | 66.2 | 2.82 |

From Table [5.10] we have found that the binding energy is maximum and equilibrium distance is minimum, when $H_2$ molecule is perpendicular on hexagon. The site with large adsorption energy and minimum equilibrium distance consider as favorable site. Therefore, the $H_2$ molecule perpendicular to the hexagonal ring is most stable than any others configuration. The calculated values of adsorption energy of $H_2$ molecule (61 meV to 69 meV) in the pure graphene sheet lies within the range of previously reported values (55 meV-80 meV) [31]. This small binding energy is due to very strong intramolecular H-H bond and its extremely small induced dipole moment, as well as the chemically inert nature of the $sp^2$ system (i.e graphene). The small binding energy implies that $H_2$ molecule can easily take out from system even at low temperature.

Further, we have studied the adsorption of $H_2$ molecule in the sodium decorated graphene system. In this study, we have adsorbed the different numbers of $H_2$

molecule on the optimized structure of the sodium-graphene system containing 18 carbon atoms and one sodium atom. The adsorption energy of the $H_2$ molecule is computed as

$$\Delta E = E_{G+Na+H_2} - E_{G+Na} - NE_{H_2} \tag{5.6}$$

where $E_{G+Na+H_2}$ is the ground state energy of the system containing graphene, sodium atom, and hydrogen molecule. $E_{G+Na}$ ground state energy of sodium decorated graphene system. $E_{H_2}$ ground state energy of the hydrogen molecule and N is number of $H_2$ molecules in the system. The positive binding energy (adsorption energy) signifies that the $H_2$ molecule bound to the system. Similarly, the binding energy per $H_2$ molecule is calculated as

$$\text{B.E. per } H_2 \text{ molecule} = \frac{\Delta E}{N}$$

The optimized structures of the adsorption of various number of hydrogen molecules on the sodium-graphene system is shown in Figure [5.36].

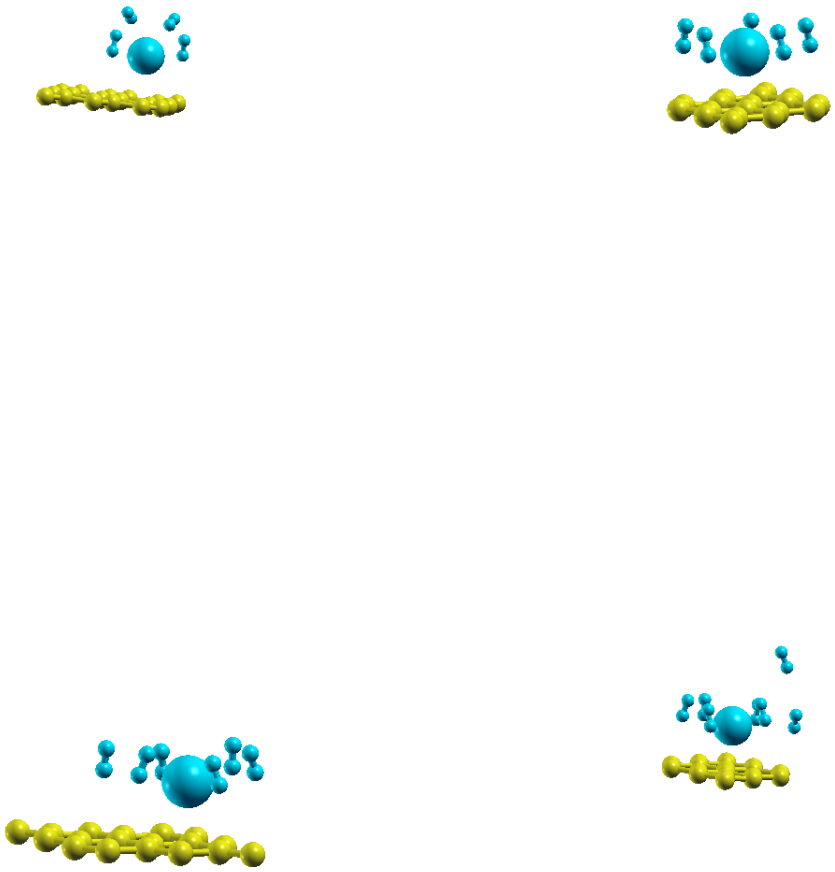

Figure 5.36: Adsorption of different numbers of hydrogen molecule in the sodium decorated graphene system.

The ground state energy, binding energy and binding energy per $H_2$ molecule are presented in the Table [5.11].

Table 5.11: The ground state energy of the Na-$H_2$-graphene system, binding energy of $H_2$ molecules and binding energy per $H_2$ molecule.

.

| Number of $H_2$ molecules | total energy (Ry) | Binding energy (eV) | Binding energy per $H_2$ molecule (eV/atom) |
|---|---|---|---|
| 1 | -299.752 | 0.023 | 0.023 |
| 2 | -302.094 | 0.174 | 0.087 |
| 3 | -304.442 | 0.405 | 0.135 |
| 4 | -306.789 | 0.628 | 0.157 |
| 5 | -309.144 | 0.960 | 0.192 |
| 6 | -311.466 | 0.829 | 0.138 |
| 7 | -313.799 | 0.869 | 0.124 |

From Table [5.11], the ground state energy of Na-$H_2$-graphene system and binding energy of $H_2$ molecule on the Na-$H_2$-graphene system continuously increases as we increase the number of $H_2$ molecules in the system. Similarly, Binding energy per $H_2$ molecule at first increases and attains the maximum value and then starts to decrease. The maximum binding energy per $H_2$ molecule is 0.192 eV/$H_2$ for the adsorption of five hydrogen molecules in Na-$H_2$-graphene system. The binding energy per $H_2$ molecule is in the range (0.023 - 0.192) eV/$H_2$, for the adsorption of one to seven numbers of $H_2$ molecule. This variation also shown in the Figure [5.37].

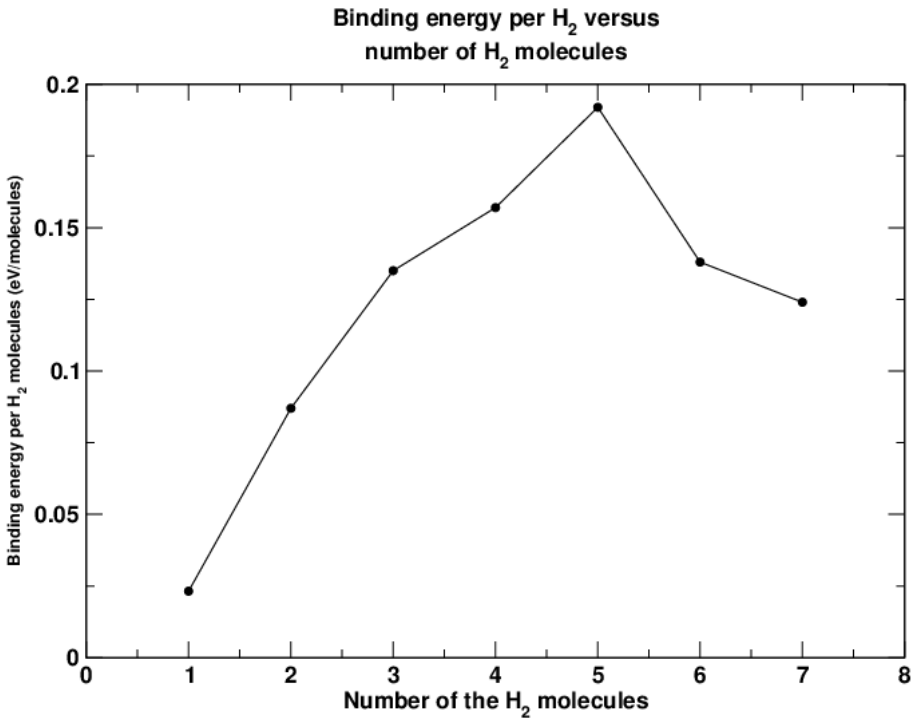


Figure 5.37: The binding energy per $H_2$ molecules is in increasing order up to certain numbers of $H_2$ molecules (up to 5 molecules) then it starts to decrease.

Figure [5.37] shows that binding energy per $H_2$ molecule at first increases and attains the maximum value 0.192 eV but when we increase the number of $H_2$ molecules beyond the 5 $H_2$ molecules, it starts to decrease. The maximum binding energy per $H_2$ molecule is 0.192 eV/$H_2$ for the adsorption of five hydrogen molecules.

A binding energy of 0.2 eV/$H_2$ is required for reversible uptake of hydrogen molecule. The estimated value of binding energy per hydrogen molecule is close with 0.2 eV/$H_2$. Also, the hydrogen storage capacity of Na decorated graphene system for the adsorption of 5 $H_2$ molecules is 4.02 wt % (weight percentage). This result is progressive towards the the DOE (Department of Energy) target (more than 6 wt %) for the practical applications [50]. This shows that Na decorated graphene has the potential applications to be used as hydrogen storage material. Therefore, Na decorated graphene can be used for hydrogen storage [48, 49].

# Chapter 6

# Conclusions and Concluding remarks

We have performed the first-principles calculations to investigate the stability, electronic and magnetic properties of pure graphene sheet and sodium decorated graphene sheet. Further, we have extended our calculations to study the adsorption of hydrogen molecules (n = 1 to 7) in the sodium decorated graphene system. The first-principles calculations have been performed within the DFT-D2 and generalized gradient approximation (GGA), including spin polarization implemented with Quantum ESPRESSO code [14]. We have used ultra-soft pseudo-potential.

The stability of pure graphene sheet has been studied with the help of ground state energy, binding energy, and binding energy per carbon atom. We have estimated the ground state energy of pure graphene sheet having 2 (unitcell), 8 ($2 \times 2$ supercell), 18 ($3 \times 3$ supercell), 32 ($4 \times 4$ supercell), and 50 ($5 \times 5$ supercell) number of carbon atoms. It is found that as the number of carbon atoms increases in the graphene sheet the ground state energy decreases linearly. From the study of the binding energy of the graphene sheets, it is found that the binding energy is a linear function of the number of carbon atoms in the graphene sheet. We have also estimated the binding energy per carbon atom as 5.723 eV, 7.789 eV, 7.901 eV, 7.904 eV, and 7.902 eV for the graphene sheets having number of carbon atoms 2, 8, 18, 32, and 50 respectively. The estimated value of binding energy per carbon atom (i.e. 7.904 eV/atom) for graphene sheet with 32 number of carbon atoms agrees within 0.60 % to the previously reported value 7.91 eV/atom by Bhattacharya et al. [29] and within 1.59 % to the value 8.03 eV/atom, reported by Oli et al. [10].

Further, we have studied the adsorption energy or binding energy of sodium (Na) atom on the pure graphene sheets with 8, 18, and 32 carbon atoms. The values of adsorption energy at different sites suggest that the hollow site is most favorable site for the adsorption of sodium atom on the graphene sheet. The equilibrium distance of sodium atom from the surface of graphene sheet is 2.40 Å, 2.32 Å, and 2.25 Å for 2×2, 3×3, and 4×4 supercell respectively. The estimated value of equilibrium distance for 4×4 supercell agrees within 1.32 % to the previously reported value 2.28 Å [27].

We have analyzed the band structure of the pure graphene and sodium decorated graphene system. In case of pure graphene, conduction band and valence band meet exactly at the Fermi level, which signifies that the pure graphene is zero band gap semiconductor. Also, we have observed that the conduction band and valence band overlapped due to the adsorption of sodium atom. Hence, sodium adsorbed graphene system can be used as conductor. We have also studied the density of states (DOS) of pure graphene and sodium adsorbed graphene. The DOS of spin up and spin down states are symmetrical in case of pure graphene which support the non magnetic nature of pure graphene but in case of sodium decorated graphene system DOS are not symmetrical, which indicates that the sodium decorated graphene system is magnetic. The change of DOS of Na-graphene system is due to the contribution of $2s$, $3p$, and $4p$ orbitals of sodium atom. The magnetic moment of isolated sodium atom is 1.00 $\mu_B$ and magnetic moment of the Na-graphene system are 0.08 $\mu_B$ and 0.24 $\mu_B$ for 3×3 and 4×4 supercell respectively. The calculated value of magnetic moment of isolated sodium atom and Na-graphene system in 4×4 supercell agrees with the previously reported values: 1.00 $\mu_B$ and 0.27 $\mu_B$ [27].

Further, we have performed the calculations to study the adsorption of hydrogen molecule on the pure graphene sheet and sodium adsorbed graphene system. The adsorption energy of a hydrogen molecule on pure graphene sheet containing 18 carbon atoms varies from 61 meV to 69 meV, which found within range of previously reported values: 55 meV to 80 meV [31]. In case of adsorption of hydrogen molecules on the sodium decorated graphene, the adsorption energy per hydrogen molecule is within range (0.023 - 0.192) eV/$H_2$ for the adsorption of one to seven $H_2$ molecules. An adsorption energy of 0.2 eV/$H_2$ is required for reversible uptake of

hydrogen molecule [50]. The observed value of adsorption energy per $H_2$ molecule is close to the required value 0.2 eV/$H_2$. Therefore, Na decorated graphene can be used for the hydrogen store.

We have studied the stability, geometrical structures and electronic properties of pure graphene and sodium adsorbed graphene. Also, we have studied the adsorption of hydrogen on pure graphene and Na-decorated graphene. We are intended to extend our work to study the adsorption of Na dimer on graphene sheet. Also, we are intended to study the adsorption of hydrogen molecule on Na dimer and other alkali metals decorated graphene to investigate the hydrogen storage capacity.

# Bibliography


[1] F. Derbyshire, *Chemistry and Physics of Carbon*, edited by L. R. Radovic, New York, (2001).

[2] A. M. Mannion, *Carbon and Its Domestication*, Springer, Dordrecht, The Nether-lands, (2006).

[3] P. R. Wallace, Phys. Rev. **71**, 622 (1947).

[4] K. S. Novoselov, A. K. Geim, S. V. Morozov, D. Jiang, M. I. Katsnelson, S. V. Dubonos, I. V. Grigorieva and A. A. Firsov, Science **306**, 666 (2004).

[5] A. K. Geim, Science **324**, 1530 (2009).

[6] M. Gibertini, A. Tomadin, M. Polini, A. Fasolino, and M. I. Katsnelson, Phys. Rev. B **81**, 125437 (2010).

[7] R. Murali, Y. Yang, K. Brenner, T. Beck, and J.D. Meindl, Appl. Phys. Lett. **94**, 243114 (2009).

[8] K. S. Novoselov, A. K. Geim, S. V. Morozov, D. Jiang, M. I. Katsnelson, Y. Zhang, I. V. Grigorieva, S. V. Dubonos and A. A. Firsov, Nature **438**, 197 (2005).

[9] K. S. Novoselov, Z. Jiang, Y. Zhang, S.V. Morozov, H.L.stormer, U. Zeitler, J.C. Maan, G.S. Boebinger, P. Kim, and A.K. Geim, Science **315**, 1379 (2007).

[10] B. D. Oli, C. Bhattarai, B. Nepal and N. P. Adhikari, Advanced nanomaterials and nanotechnology, **143**, 515 (2013).

[11] P. Chen, X. Wu, J. Lin, and K. L. Tan, Science **285**, 91 (1999).

[12] J. M. Thijssen, *Computational Physics*, Cambridge University Press, Cambridge, (1999).

[13] S. M. Blinder, J. Phys. **6**, 33 (1965).

[14] P. Giannozzi, S. Baroni, and N. Bonini, M. Calandra, R.Car, C. Cavazzoni, D. Ceresoli, G. L. Chiarotti, M. Cococcioni, I. Dabo11, A. D. Corso1, S.de Gironcoli, S. Fabris, G. Fratesi, R. Gebauer, U. Gerstmann, C. Gougoussis, A. Kokalj, M. Lazzeri, L. M. Samos1, N. Marzari, F. Mauri, R. Mazzarello, S. Paolini, A. Pasquarello, L. Paulatto, C. Sbraccia1, S. Scandolo, G. Sclauzero, A. P. Seitsonen, A. Smogunov, P. Umari and R. M. Wentzcovitch, J. Phys. Condens. Matter **21**, 395502 (2009).

[15] A. R. Leach, *Molecular Modelling Principles and Applications*, 2nd ed., Pearson Education Ltd., India (2010).

[16] L. H. Thomas, Proc. Camb. Philos. Soc. **23**, 542 (1927).

[17] E. Fermi, Z. phys. **48**, 73 (1928).

[18] R. M. Dreizler and E. K. U. Gross, *Density Functional Theory*, Springer-Verlag, Berlin (1990).

[19] P. Hohenberg, W. Kohn, Phys. Rev. **136**, B864 (1964).

[20] S. Grimme J. Comput. Chem. **25**, 1463 (2004).

[21] M. Piacenza and S. Grimme, J. Chem. Phys. **6**, 1554 (2005).

[22] M. Parac, M. Etinski, M. Peric and S. Grimme, J. Comput. Chem. **1**, 1110 (2005).

[23] S. Grimme, J. Comput. Chem. **27**, 1787 (2006).

[24] S. Baroni, S.de Gironcoli, A.D. Corso, and P. Giannozzi, Rev. Mod. Phys. **73** (2001).

[25] W. Kohn and L.J. Sham, Phys. Rev. **140**, A1133 (1965).

[26] J. P. Perdew, K.Burke, and M.Ernzerhof, Phys. Rev. Lett. **77**, 3865 (1996).

[27] K. T. Chan, J. B. Neaton, and Marvin L. Cohen, Phys. Rev. B **77**, 235430 (2008).

[28] P. V C Medeiros, F de Brito Mota, Artur J S Mascarenhas and C. M C de Castilho, IOP Sc. **21**, 115701 (2010) .

[29] A. Bhattacharya, S. Bhattacharya, C. Majumder, G. P. Das, J. Phys. Chem. C **114**, 10297 (2010).

[30] M. Caragiu and S. Finberg, J. Phys. Condens. Matter **17**, R995 (2005).

[31] Y. K. Kwon, J. Korean Phys. Soc. **57**, 778 (2010).

[32] B. K. Agarwal and H. Prakash, *A text book of Quantum Mechanics*, 7th ed., PHL private limt., New Delhi, (1997).

[33] M. S. Dresselhaus, G. Dresselhaus, and P. C. Eklund, *Science of Fullerenes and Carbon Nanotubes* (Academic, San Diego, 1996).

[34] D. Vanderbilt, Phys. Rev. B **41**, 7892 (1990).

[35] D. Vanderbilt, Phys. Rev. B **32**, 8412 (1985).

[36] N. Troullier and J. L. Martins, Phys. Rev. B **43**, 1993 (1991).

[37] A. H. Castro Neto, *The carbon new age* , Department of Physics, Boston University, 590 Commmonwelth Avenue, Boston, MA 02215 USA.

[38] R. D. Diehl and R. McGrath, J. Phys. Condens. Matter **9**, 951 (1997).

[39] Z. Zhu, G. Lu, and F. Wang, J. Phys. Chem. B **109**, 7923 (2005).

[40] F. Valencia, A. Romero, F. Ancilotto, and P. Silvestrelli, J. Phys. Chem. B **110**, 14832 (2006).

[41] K. Rytknen, J. Akola, and M. Manninen, Phys. Rev. B **75**, 075401 (2007).

[42] F. Ancilotto and F. Toigo, Phys. Rev. B **47**, 13713 (1993).

[43] L. Lou, L. sterlund, and B. Hellsing, J. Chem. Phys.**112**, 4788 (2000).

[44] J. S. arellano, L. M. Molina, A. Rubio, M. J. Lopez and J. A. Alonso, J. Chem. Phys. **117**, 2281 (2002).

[45] C. Kittel, *Introduction to Solid Sate Physics*, 7th ed. (Wiley, New Delhi, 2004).

[46] R. M. Martin., *Electronic structure:Basic Theory and Practical Methods* (Cambridge University Press, United Kingdom, 2004).

[47] N. W. Ashcroft and N. D. Mermin., *Solid State Physics* (New York, 1976).

[48] B. Chen, B. Li, and L. Chen, Appl. Phys. Lett. **93**, 043104 (2008).

[49] K. R. S. Chandrakumar and S. K. Ghosh, Nano Lett. **8**, 13 (2008).

[50] K. S. Kim, Y. Zhao, H. Jang, S. Y. Lee, J. M. Kim, J. H. Ahn, P. Kim, J. Y. Choi, and B. H. Hong, Nature (London) **457**, 706 (2009).